



## Ion-exchange equilibrium of cesium/hydrogen ions on zirconium molybdate and zirconium iodomolybdate cation exchangers

B. El-Gammal\*, G.M. Ibrahim<sup>1</sup>, S.H. El-Kholy, S.A. Shady

Hot Laboratories Center, Atomic Energy Authority, P. No. 13759, Cairo, Egypt, email: [belalelgammal@hotmail.com](mailto:belalelgammal@hotmail.com) (B. El-Gammal)

Received 12 February 2013; Accepted 22 May 2014

### ABSTRACT

The ion-exchange behavior of  $^{134}\text{Cs}^+$  onto zirconium molybdate (ZM) and zirconium iodomolybdate (ZIM) under batch conditions was achieved in different media. Acetic acid and EDTA were used as organic ligands; whereas sodium chloride and sodium nitrate were used as inorganic media containing  $\text{Na}^+$  as competing ion for  $^{134}\text{Cs}^+$  adsorption on ZM and ZIM. Based on Davis and Debye–Huckel Equations, the activities and the activity coefficients of the corresponding concentrations were calculated. Different isothermal models were used to express the effect of activity on the amount of  $^{134}\text{Cs}^+$  sorbed onto ZM and ZIM. The best-fitted adsorption isotherm models were in the order of BET > Freundlich > Temkin > Sips > Langmuir in case of  $^{134}\text{Cs}^+/\text{ZM}$ , while the order was Temkin > Freundlich > BET > Langmuir > Sips in case of  $^{134}\text{Cs}^+/\text{ZIM}$ . Traditional surface complexation models (SCMs) could not account for the sorption of  $^{134}\text{Cs}^+$  onto ZM and ZIM in presence of different ligands or competing ions; the 2-pK basic Stern model and the triple-layer model (TLM) was not satisfactory, due to the high number of adjustable parameters involved in these model variations. Furthermore, a purely diffuse layer model (DLM) generally gave the poorest fit to experimental data when combined with the 1-pK approach and was only slightly better when combined with the 2-pK formalism. Therefore, a new model, surface site competition complexation model (SSCCM) was developed by G. M. Ibrahim and B. El-Gammal, based on 2-pK DLM to test several sets of data, including those containing ligand complexes and competing cations. The theoretical basis, postulates, the model equations, and the calculations were discussed in detail. The new SSCCM succeeded in explanation of the marked sets of sorption data in distinctive ionic strengths giving rise to the different activities, species, and their distributions in existence of both the organic complexing ligands as acetic acid and EDTA and sodium as monovalent competing ion. The SSCCM explained the results of the solubility's of the inorganic species by calculation of their logarithmic ionic activity products and the corresponding saturation indices. In addition, the surface charges and surface potentials were computed. Since the calculations in the SSCCM are based on the activities, the model could predict the real formation constants, and in turn, it could be precisely used to calculate the different thermodynamic parameters. Negative free energy changes indicate the spontaneous nature of the sorption process, while the positive values for both enthalpy change and entropy change indicates that the sorption process is entropy directed.

\*Corresponding author.

<sup>1</sup>Present address: King Khaled University, Bisha Branch, Saudi Arabia.

**Keywords:**  $^{134}\text{Cs}^+$ ; Zirconium molybdate; Zirconium iodomolybdate; Distribution Coefficient; Isothermal models; Surface site competition complexation model; Thermodynamics

## 1. Introduction

The operations of nuclear power plants as well as nuclear fuel reprocessing and radioisotopes production facilities generate large amounts of high-level radioactive wastes. The major contaminants of these wastes are fission products and actinides. The recovery of valuable elements, lanthanides, and actinides from high-level nuclear wastes is an area of worldwide concern. Among the main fission products released, cesium radioisotopes stand as the most important fission products because of their high fission yield, long half-life ( $^{137}\text{Cs}$  ( $T_{1/2} \sim 30.17$  y),  $^{135}\text{Cs}$  ( $T_{1/2} \sim 2.3 \times 10^6$  y),  $^{134}\text{Cs}$  ( $T_{1/2} \sim 2.06$  y)), and serious environmental impacts [1]. Radioactive cesium contamination is of serious social and environmental concerns. It presents serious threat to human health and environment because it is a strong gamma emitter and has high solubility that enhances its migration through groundwater to the biosphere [2]. Besides, cesium can be easily incorporated in terrestrial and aquatic organisms because of its chemical similarity to potassium. The solubility/mobility of cesium was amounted up to 186, 209, 261, and 400 g/100 g of water at  $\sim 20^\circ\text{C}$  for  $\text{CsCl}$ ,  $\text{CsHCO}_3$ ,  $\text{Cs}_2\text{CO}_3$ , and  $\text{CsOH}$ , respectively. Besides its high mobility, cesium can travel in airborne dust particles and can be present in food and water. Therefore, the migration of  $^{137}\text{Cs}$  has become a key criterion of performance assessment in radioactive waste repository construction. In addition, cesium radionuclides are considered potentially dangerous to human health, if exposed via ingestion route, cesium is 100% absorbed from the gut to the body and is distributed fairly uniformly throughout the body's soft tissues. Actually,  $^{137}\text{Cs}$  is the major cause of thyroid cancer in Belarus, which took 70% of the fallout from the Chernobyl nuclear disaster [1,2].

Adsorption of  $^{134}\text{Cs}^+$  ions by ion-exchange to mineral phases in solution is of great importance in the regulation of many trace metals in the environment. Among the most common inorganic ion-exchangers including hydroxides, oxyhydroxides, and clay minerals, metal hydroxides have the highest affinity for inorganic ions in solution due to their high specific surface area (SSA), surface charge, and reactive site density [3]. While the adsorption behavior of  $^{134}\text{Cs}^+$  on metal molybdates has not been extensively studied, it is understood that both aqueous complexation and potential ternary complex formation can influence the

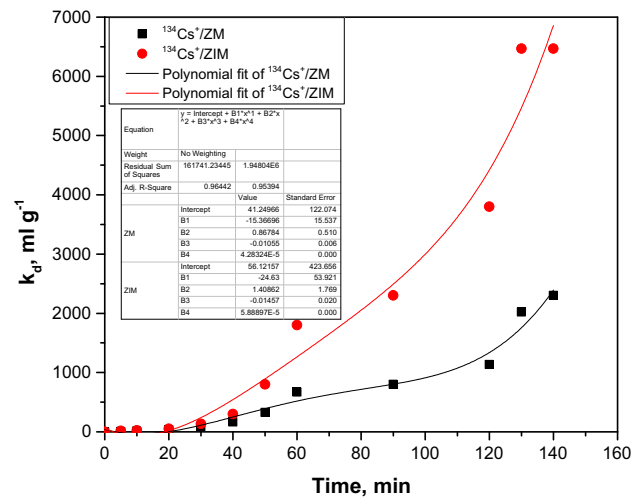


Fig. 1. Distribution coefficient plots of  $^{134}\text{Cs}^+$  onto ZM and ZIM as a function of contact time.

extent of adsorption to mineral surfaces [4]. Numerous experimental and modeling studies for metal ion adsorption have been performed and the data obtained has been fit to a variety of adsorption isotherm or surface complexation models (SCMs) [5,6]. SCM that allow formation of inner- and outer-sphere complexes between surface hydroxyl groups and

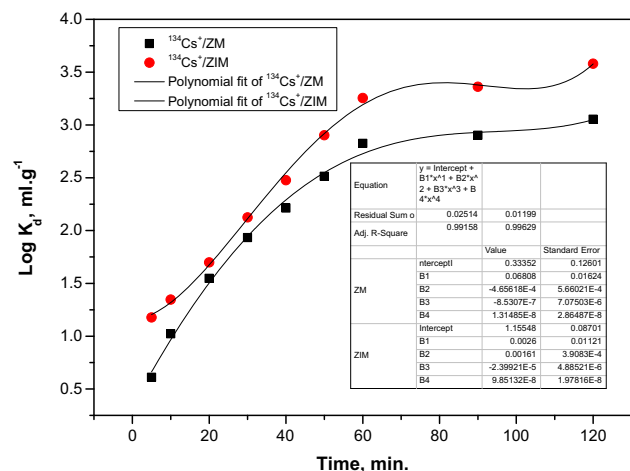


Fig. 2. Logarithmic plots of distribution coefficient of  $^{134}\text{Cs}^+$  onto ZM and ZIM as a function of contact time.

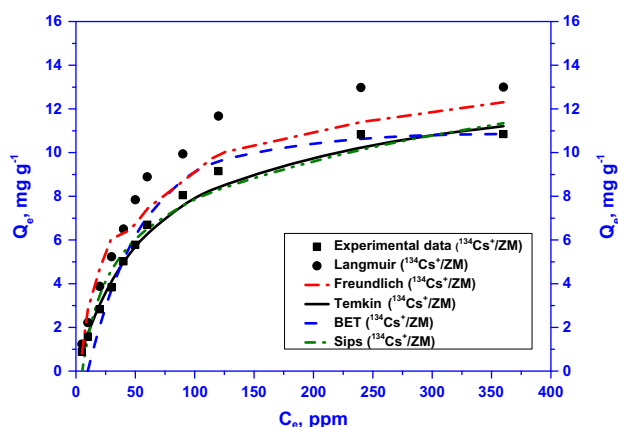


Fig. 3. Sorption isotherms of  $^{134}\text{Cs}^+$  onto ZM using different models.

complexing aqueous ions offer the greatest potential for describing metal adsorption because they have the ability to account for the impacts of pH, ionic strength, and ternary complex formation. There are a number of SCM that differ in their description of the interfacial region both with respect to the description of the relationship between surface charge and potential, and the location of the sorbed species [7]. The Non Electrostatic Model and the Diffuse Layer Model (DLM) offer simplistic descriptions of the double layer region that require minimal parameter estimation but only allow formation of inner-sphere complexes. Both the Triple Layer Model (TLM) and the Charge Distribution Multi-Site Complexation (CD-MUSIC) model provide a more complete description of the interfacial region and the means to account for both inner- and outer-sphere complexation as well as ligand exchange that

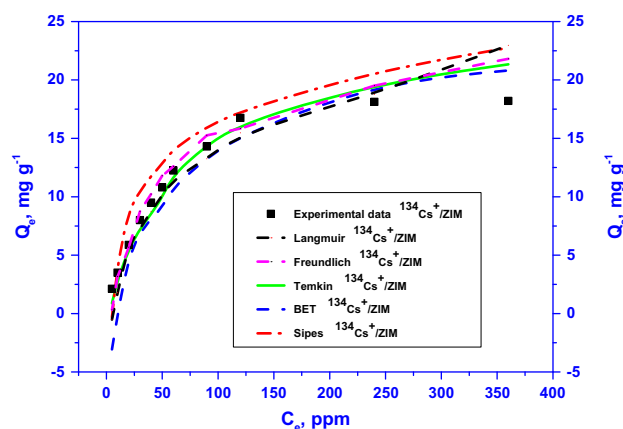


Fig. 4. Sorption isotherms of  $^{134}\text{Cs}^+$  onto ZIM using different models.

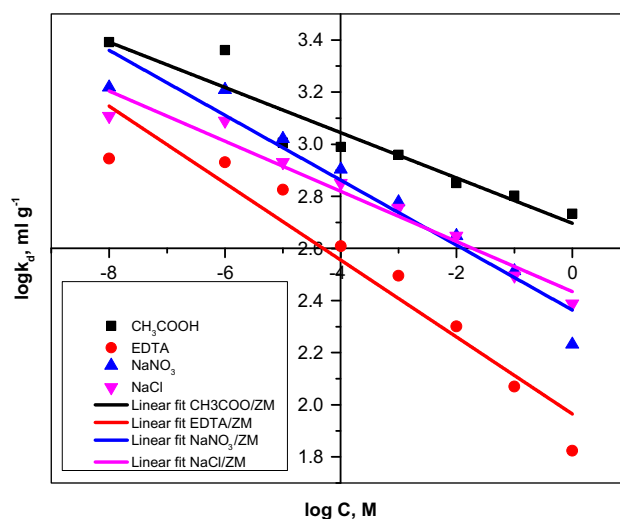


Fig. 5. Ibrahim-El-Gammal SSCCM plots for  $^{134}\text{Cs}^+$ /ZM system.

is consistent with spectroscopic measurements [8]. The CD-MUSIC model can be differentiated from the TLM by three major characteristics; representation of surface acidity, placement of ions, and charge in electrostatic planes, and representation of reactive surface adsorptions sites [9].

Although the aforementioned models could describe the metal sorption in different situations, they failed to study the screening effect caused by the presence of some complexing ligands or competing ions [5–9]. The efforts utilizing the classical 2-pK, CCM, and TLM models were unable to predict

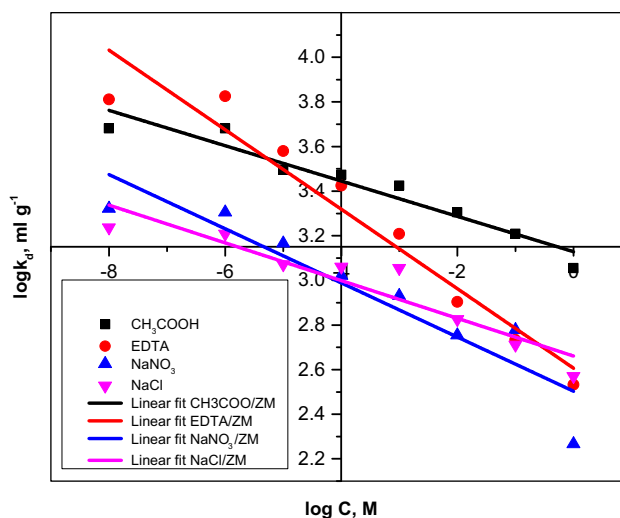


Fig. 6. Ibrahim-El-Gammal SSCCM plots for  $^{134}\text{Cs}^+$ /ZIM system.

$^{134}\text{Cs}^+$  adsorption adequately or did not employ surface species that are consistent with molecular scale analyses. Thus, the development of a more accurate SCM that incorporates ligand complexation effects or competing ions with the main ion adsorption is warranted. In this study, a new surface site competition complexation model (SSCCM) describing  $^{134}\text{Cs}^+$  adsorption and aqueous speciation has been developed over a range of experimental conditions to provide a tool for predicting the fate and transport of  $^{134}\text{Cs}^+$  down gradient at zirconium molybdate (ZM) and zirconium iodomolybdate (ZIM) sites. Competitive  $^{134}\text{Cs}^+$  adsorption on ubiquitous minerals such as ZM and ZIM has been evaluated over a range of experimental conditions.

## 2. Experimental

### 2.1. Starting chemicals and solutions

Analytical rank chemicals were used in different procedures; concentrated  $\text{HNO}_3$ ,  $\text{HCl}$ ,  $\text{NH}_4\text{OH}$ , and pH buffers (BDH grade chemicals) were used in pH adjustments with no further purification. Molybdenum(VI) in nitric acid (from 69% w/v nitric acid, Prolabo, France) was prepared at concentrations by dissolving reagent grade (Acros, France) molybdenum(VI) oxide powder. Zirconium(IV) in nitric acid was separately prepared at concentrations by dissolving reagent grade zirconium oxychloride ( $\text{ZrOCl}_2 \cdot 8\text{H}_2\text{O}$ ), (Merck, Germany) after having determined the water content by thermogravimetry. Synthetic stock solutions of  $\text{NaCl}$ ,  $\text{NaNO}_3$ , acetic acid ( $\text{C}_2\text{H}_4\text{O}_2$ ), citric acid ( $\text{C}_6\text{H}_8\text{O}_7$ ), and  $\text{HNO}_3$  were prepared at different concentrations in deionized water from  $10^{-8}$  to 1 M solution.

### 2.2. Adsorbent materials

#### 2.2.1. Preparation of zirconium molybdate

ZM was synthesized by the same procedure reported earlier [10–14], but with different molar ratios of the reactants, by dissolving molybdenum trioxide ( $\text{MoO}_3$ ) in sodium hydroxide solution  $\text{NaOH}$  ( $2 \text{ mol L}^{-1}$ ); afterwards the sodium molybdate ( $\text{Na}_2\text{MoO}_4$ ) solution was neutralized with nitric acid  $\text{HNO}_3$  ( $2 \text{ mol L}^{-1}$ ) up to pH 4.5. The consequent sodium molybdate solution is subsequently added to zirconium(IV)oxychloride solution  $\text{ZrOCl}_2 \cdot 8\text{H}_2\text{O}$  ( $20 \text{ mg mL}^{-1}$ ) and heated at  $50^\circ\text{C}$  (molar ratio of  $\text{Zr}/\text{Mo} \approx 1.6$ ) with constant stirring for 30 min. Then the colloidal mixture formed is of pH 1–2 so the sodium hydroxide solution ( $2 \text{ mol L}^{-1}$ ) must be added to the colloidal mixture up to pH 5. The colloidal

mixtures were filtered, and the precipitate was washed with demineralized water (DMW), dried at  $105^\circ\text{C}$  in a drying oven, then finally ground and sieved to obtain the different mesh sizes.

#### 2.2.2. Preparation of zirconium iodomolybdate

With a different way to that cited in literature [15], ZIM could be synthesized in the laboratory, by synthesis of iodic acid  $\text{HIO}_3$  because of reaction between Iodine and chlorine in aqueous phase. To avoid combustion, the acid was gently added to  $\text{KOH}$  in fume-hood, so that potassium iodate,  $\text{KIO}_3$  was produced. A mixture of 0.5 M potassium iodate and 0.5 M sodium molybdate solution to 0.5 M zirconium(IV) oxychloride solution was established with continuous stirring to obtain a gel. The desired pH was adjusted by adding dilute  $\text{HCl}$  or  $\text{NH}_3$  solutions. The gel was aged in the mother liquor for 24 h at room temperature and filtered under suction. The excess acid was removed by washing with DMW, and it was kept in an oven at  $50^\circ\text{C}$  for drying. The dried product was then cracked into small granules by putting in DMW, which was converted into the H-form by treating with 1 M  $\text{HNO}_3$  for 24 h at room temperature. Different groups such as molybdate ( $\text{O}^-\text{MoO}_3$ ) and iodate ( $\text{O}^-\text{IO}_2$ ) would be converted to the protonated forms of  $\text{MoO}_4\text{H}_2$  and  $\text{IO}_3\text{H}$ , respectively. The material was finally washed with DMW to remove any excess of acid [16–18].

#### 2.2.3. Characterization of ZM and ZIM

The based molybdate exchangers were characterized by advanced analytical tools. Simultaneous DTA–TGA system, type DTA–TGA–50, Shimadzu, Japan, was used to measure phase transformations and weight losses from the sample, respectively, at a heating rate of  $10^\circ\text{C min}^{-1}$  under nitrogen gas to avoid thermal oxidation of the ZM and ZIM powders.

Powder X-ray diffraction (XRD, model XD610, Shimadzu, Japan) data used for least-squares refinements of lattice parameters were recorded on an X-ray diffractometer, at room temperature, using Bragg–Brentano geometry, with a back monochromatic  $\text{Cu K}\alpha$  radiation. Samples were ground and mounted on a flat sample plate. The diffraction pattern was scanned over the angle range  $4\text{--}90$  ( $2\theta$ ) in step of  $0.031$  ( $2\theta$ ) and a counting time of 10 s per step. The unit-cell parameters were refined by a least-squares procedure.

Perkin Elmer FTIR, model BXII, USA, in the range  $500\text{--}4,000 \text{ cm}^{-1}$  was cast off to identify the IR spectrum

of the different molybdate-based exchangers by activating the disc technique. In this concern, every sample was thoroughly mixed with KBr as a matrix, and the mixture was ground and then compressed with a special press to give a disc of standard diameter.

Laser diffraction particle size analyzer (SALD 2001, Shimadzu, Japan) was used to distinguish between the different mesh sizes obtained as well as their distributions.

Textural characterizations of the ZM and ZIM were carried out by N<sub>2</sub> adsorption at 77 K using Autosorb I, supplied by Quantachrome Corporation, USA. The BET (N<sub>2</sub>, 77 K) is the most usual standard procedure used when characterizing these exchangers.

### 2.3. Ion exchange studies

#### 2.3.1. Distribution of <sup>134</sup>Cs<sup>+</sup> on different exchangers

The sorption of <sup>134</sup>Cs<sup>+</sup> on ZMB and ZIMB and the ramification of the reaction media under various conditions of ligand concentrations and pH was evaluated by the distribution coefficient,  $K_d$ . The estimation of  $K_d$  was measured depending on two separate methods:

The first routine was used to calculate the difference between the total radionuclide activity of <sup>134</sup>Cs<sup>+</sup> added, and that left in the suspension. In many experiments, some ZMB, ZIMB, and/or <sup>134</sup>Cs<sup>+</sup> sorbed to it, could be adhered to the tube walls. This led to an overestimation of the adsorption on the tube walls. The logarithmic distribution coefficients were overestimated by about 0.87; correction was made so that the <sup>134</sup>Cs<sup>+</sup> is estimated on ZMB and ZIMB rather than the tube walls.

In the latter procedure, the tube was leached with acid after being washed with water and the amount of <sup>134</sup>Cs<sup>+</sup> lost during washing off in this method led to an underestimation; log  $K_d$  decreased at 0.06. Adsorption to the tube walls was taken into account in the calculations, because it had a considerable effect on the  $K_d$ , except for when a ligand was present or when Log  $K_d$ —was used in calculation in the system according to the following Equation.

$$K_d = \frac{(C_i - C_f)V}{C_f W} \quad (1)$$

where  $C_i$  and  $C_f$  represent the initial and equilibrated concentrations of the given metal ions in solution, and  $V$  (mL) and  $W$  (g) are the volume of solution and the mass of adsorbent, respectively.

In both procedures, replication of experiments was conducted for estimation of the uncertainty of the

results in presence and absence of ligand at different concentrations. The standard deviation of the results was about 0.091. The same procedures were carried out using organic materials such as acetic acid and EDTA as complexing agents and sodium chloride as well as sodium nitrate of various concentrations as competing ions.

#### 2.3.2. Loading of <sup>134</sup>Cs<sup>+</sup> on ZM and ZIM

Batch experiments were conducted to investigate the adsorption of <sup>134</sup>Cs<sup>+</sup> on ZMB and ZIMB from its aqueous solution. 1 g of ZM or ZIM was added into 25 mL colorimetric tube containing the applicable concentrations at a pH value of 5.0 at 25°C. Then the mixture was shaken vigorously for 10 min and the adsorption was maintained for a certain moment. After centrifugation, the residual amount of <sup>134</sup>Cs<sup>+</sup> on ZMB and ZIMB in the supernatant was assayed radiometrically using NaI(Tl) scintillation detector connected to an ORTEC assembly (Nuclear Enterprises), USA. The adsorption ratio ( $E\%$ ), absorption capacity  $Q_e$  (mg g<sup>-1</sup>) at equilibrium, and adsorption amount at time  $t$  (min)  $Q_t$  (mg g<sup>-1</sup>) were calculated as follows:

$$E\% = \frac{C_0 - C_e}{C_0} \times 100\% \quad (2)$$

$$Q_e = \frac{(C_0 - C_e)V}{W} \quad (3)$$

$$Q_t = \frac{(C_0 - C_t)V}{W} \quad (4)$$

where  $C_0$  (mg L<sup>-1</sup>),  $C_e$  (mg L<sup>-1</sup>) and  $C_t$  (mg L<sup>-1</sup>) are concentrations of <sup>134</sup>Cs<sup>+</sup> at initial, equilibrium, and time  $t$  (min) states, respectively. Later on, these Equations could be used in describing the sorption isotherms.

## 3. Results and discussion

### 3.1. Characterization of the exchangers

#### 3.1.1. Characterization of ZM

In similarity to- and After- El-Gammal and Shady [12], the XRD patterns of ZM heated at different drying temperatures (50, 200, 400, 600, and 850°C), revealed that ZM was amorphous but increasing the drying temperatures, especially at 600 leads to the formation of ZrOMoO<sub>4</sub> crystalline phase with significant

improvement of crystallinity at 850°C with no phase changes in the sample.

Also, the infrared spectra ZM showed a wide band at  $\approx 2,500\text{--}3,600\text{ cm}^{-1}$  due to strong inter- and intra-molecular hydrogen bonding. Another band at  $600\text{--}900\text{ cm}^{-1}$  was assigned to M–O interaction vibrations [19]. However, the band around  $1,640\text{ cm}^{-1}$  was due to M–OH vibration, which could be ascribed to  $\delta$  M–OH.

The DTA data of ZM revealed an endothermic peak at about 109°C, concurs to loss of free water. The weight loss continued up to 600°C, due to removal of the crystalline water. The small exothermic peak at 588°C, corresponds to the crystallization of  $\text{ZrO}_2$  and  $\text{MoO}_3$  to form  $\text{ZrOMoO}_4$ . The total water content obtained from TGA measurements and calcination of the prepared materials was found to be 16.4 wt-%.

From the BET measurements, the surface area,  $S_{\text{BET}}$ , the total pore volumes estimated from the volume of  $\text{N}_2$  adsorbed at  $p/p^\circ = 0.95$ ,  $V_t$ , and the average pore radius,  $D_{\text{avr}}$ , were found to be  $175.36\text{ m}^2\text{ g}^{-1}$ ,  $0.23\text{ cm}^3\text{ g}^{-1}$ , and  $12.36\text{ \AA}$ , respectively, for ZM cation exchanger.

### 3.1.2. Characterization of ZIM

Chemically, ZIM was formulated as  $\text{ZrO}(\text{OH})_2(\text{IO}_3)(\text{MoO}_4) \cdot n\text{H}_2\text{O}$ , which was naturally amorphous granules as indicated by its XRD.

Simultaneous DTA-TGA results indicated a weight loss by 14–19% within the temperature range until 150°C and augmented by an endothermic peak at  $\sim 120^\circ\text{C}$ . However, no peaks were observed up to 360°C, as there was no phase change at this temperature. At higher temperatures, an endothermic peak was revealed at  $\sim 380^\circ\text{C}$  that is attributed to the transformation to  $\text{MoO}_4$  and accompanied by weight loss at the same temperature due to condensation of internal water molecules to get this phase. The exothermic peak revealed further crystallization to  $\text{ZrIMoO}_8$  at 590°C, with no weight loss. The thermograms clarify that increasing the iodate content in prepared exchanger decreases its caloric stability and approves the stability of the synthesized precursors up to 350°C. The thermal stability of these adsorbents reflected their surface structure stability under high temperature; the damage of the surface structure resulted in the decrease of SSA. The obtained  $S_{\text{BET}}$ ,  $V_t$ , estimated from  $\text{N}_2$  adsorbed at  $p/p^\circ = 0.95$  were about  $226.48\text{ m}^2\text{ g}^{-1}$ ,  $0.524\text{ cm}^3\text{ g}^{-1}$ , and  $3.27\text{ \AA}$ , respectively.

### 3.2. Calculation of the activity coefficients

The activity coefficient is an important parameter for detection of the non-fictitious equilibrium distribution coefficient between the aqueous and solid phases, and in turn, an actual determination of the thermodynamic parameters is expected. In any A–B binary system, the preference of the adsorbent for the two ions could be expressed by the selectivity coefficient,  $K_{c(A-B)}$ .

$$K_{c(A-B)} = \frac{\bar{E}_A \cdot C_B \cdot \gamma_{\pm B\text{NO}_3}}{\bar{E}_B \cdot C_A \cdot \gamma_{\pm A\text{NO}_3}} \quad (5)$$

where  $\gamma_{\pm}$  is the mean activity coefficient of the electrolytes in the solution,  $C_A$  and  $C_B$  are the molar solution concentrations of the competing ions A and B in nitrate medium, respectively, whereas, the under barred  $E_A$  and  $E_B$  are the equivalent fractions of the same ions in the solid phase.

From Eq. (1), the mean activity coefficient is considered as an important factor that can be represented by the Debye–Hückel equation (6) [20].

$$\log \gamma_{\pm} = -\frac{X Z_+ Z_- I^{0.5}}{1 + Y a_i I^{0.5}} \quad (6)$$

where X and Y are Debye–Hückel constants (they were taken as  $0.5115\text{ (L mol}^{-1})^{1/2}$  and  $3.29 \times 10^7\text{ L}^{1/2}/\text{cm mol}^{1/2}$ , respectively),  $Z_+$  and  $Z_-$  are the charge values of the positive and negative ions, respectively,  $a_i$  is the closest distance of ion approach ( $1.67 \times 10^{-8}\text{ cm}$ ), which is smaller than that reported earlier for the identical cesium salt in aqueous solution in the equivalent conditions [21]. However, the ionic strength of a given solution, I, can be expressed as:

$$I = \frac{1}{2} \sum c_i z_i^2 \quad (7)$$

Since the ratio of the mean activity coefficients of the two exchanging ions are usually fractions between 0.99 and 1, Debye–Hückel theory could be used in determination of the thermodynamic equilibrium constant,  $K_e$ , according to the following relationship [22]:

$$\ln K_e = \int_0^1 \ln K_{c(A-B)} d\bar{E}_A \quad (8)$$

Table 1

Concentrations and activities ( $\text{mol L}^{-1}$ ) of aqueous inorganic and organic species at  $\text{pH}=0.5$  and  $I=0.2137$  from  $10^{-3}$  M  $\text{CsNO}_3$  and  $1 \times 10^{-8}$  M acetate solution

| Component                    | Concentration | Activity | Log activity |
|------------------------------|---------------|----------|--------------|
| Acetate <sup>-1</sup>        | 7.82E-13      | 5.81E-13 | -12.236      |
| Cs <sup>+</sup>              | 0.000999      | 0.000743 | -3.129       |
| Cs-Acetate (aq)              | 3.12E-16      | 3.28E-16 | -15.485      |
| CsNO <sub>3</sub> (aq)       | 5.5E-07       | 5.78E-07 | -6.238       |
| H <sup>+</sup>               | 0.42534       | 0.31623  | -0.5         |
| H-Acetate (aq)               | 1E-08         | 1.05E-08 | -7.979       |
| NO <sub>3</sub> <sup>-</sup> | 0.000999      | 0.000743 | -3.129       |
| OH <sup>-</sup>              | 4.28E-14      | 3.18E-14 | -13.497      |

Table 2

Species distribution of aqueous inorganic and organic species at  $\text{pH}=0.5$  and  $I=0.2137$  from  $10^{-3}$  M  $\text{CsNO}_3$  and  $1 \times 10^{-8}$  M acetate solution

| Component                    | % of total concentration | Species name                 |
|------------------------------|--------------------------|------------------------------|
| Acetate <sup>-1</sup>        | 99.992                   | H-Acetate (aq)               |
| Cs <sup>+</sup>              | 99.945                   | Cs <sup>+</sup>              |
|                              | 0.055                    | CsNO <sub>3</sub> (aq)       |
| NO <sub>3</sub> <sup>-</sup> | 99.945                   | NO <sub>3</sub> <sup>-</sup> |
|                              | 0.055                    | CsNO <sub>3</sub> (aq)       |

When 0.001 M  $\text{CsNO}_3$  natural solutions are prepared in bidistilled water, both theoretical and calculated pH values were semi-identical as 6.998 and 6.997. This similarity is expected as both summations of the negatively charged nitrate anions, and the positively charged cesium cations are identically recorded as  $9.9 \times 10^{-4} \text{ mol kg}^{-1}$ . On the other hand, the preparation of 0.001 M  $\text{CsNO}_3$  led to a resultant pH of the system = 6.98; the equilibrium concentration was distributed between  $99.9 \times 10^{-4}$  M as free Cs<sup>+</sup> and NO<sub>3</sub><sup>-</sup> ions and  $9.71 \times 10^{-7}$  M combined CsNO<sub>3</sub> ion pair.

According to Eqs. (5) and (6), the cationic and anionic charges were equally distributed between the main cationic and anionic species, respectively in the

Table 3

Mass distribution of aqueous inorganic and organic species at  $\text{pH}=0.5$  and  $I=0.2137$  from  $10^{-3}$  M  $\text{CsNO}_3$  and  $1 \times 10^{-8}$  M acetate solution

| Component                    | Total dissolved | % dissolved | Total sorbed |
|------------------------------|-----------------|-------------|--------------|
| Acetate <sup>-1</sup>        | 1E-08           | 100         | 0            |
| Cs <sup>+</sup>              | 0.001           | 100         | 0            |
| H <sup>+</sup>               | 0.42534         | 100         | 0            |
| NO <sub>3</sub> <sup>-</sup> | 0.001           | 100         | 0            |

Table 4

Concentrations and activities ( $\text{mol L}^{-1}$ ) of aqueous inorganic and organic species at  $\text{pH}=0.5$  and  $I=0.2137$  from  $10^{-3}$  M  $\text{CsNO}_3$  and 1 M acetate solution

| Component                    | Concentration | Activity   | Log activity |
|------------------------------|---------------|------------|--------------|
| Acetate-1                    | 7.9444E-06    | 5.9063E-06 | -5.229       |
| Cs <sup>+</sup>              | 9.9949E-04    | 7.4308E-04 | -3.129       |
| Cs-Acetate (aq)              | 3.1695E-09    | 3.3293E-09 | -8.478       |
| CsNO <sub>3</sub> (aq)       | 5.5044E-07    | 5.7820E-07 | -6.238       |
| H <sup>+</sup>               | 4.2534E-01    | 3.1623E-01 | -0.500       |
| H-Acetate (aq)               | 1.0161E-01    | 1.0674E-01 | -0.972       |
| NO <sub>3</sub> <sup>-</sup> | 9.9949E-04    | 7.4309E-04 | -3.129       |
| OH <sup>-</sup>              | 4.2829E-14    | 3.1842E-14 | -13.497      |

Table 5

Species distribution of aqueous inorganic and organic species at  $\text{pH}=0.5$  and  $I=0.2137$  from  $10^{-3}$  M  $\text{CsNO}_3$  and 1 M acetate solution

| Component                    | % of total concentration | Species name                 |
|------------------------------|--------------------------|------------------------------|
| Acetate <sup>-1</sup>        | 99.992                   | H-Acetate (aq)               |
| Cs <sup>+</sup>              | 99.945                   | Cs <sup>+</sup>              |
|                              | 0.055                    | CsNO <sub>3</sub> (aq)       |
| NO <sub>3</sub> <sup>-</sup> | 99.945                   | NO <sub>3</sub> <sup>-</sup> |
|                              | 0.055                    | CsNO <sub>3</sub> (aq)       |

level of  $9.99 \times 10^{-4} \text{ molecule kg}^{-1}$ ; charge difference was kept at zero. The activity coefficients of both species were found as 0.9649.

At pH 5, the charge difference was about 99.89 molecule  $\text{kg}^{-1}$  at 0.2137 ionic strength. Therefore, the activity coefficients of both species were lowered to 0.74. This may be attributed to the changes encountered in the equilibrium concentrations of the species; the molarities of Cs<sup>+</sup>, NO<sub>3</sub><sup>-</sup>, and CsNO<sub>3</sub> were found to be  $9.99 \times 10^{-4}$ ,  $9.99 \times 10^{-4}$ , and  $5.5 \times 10^{-7}$  M, respectively. In contrast to the natural cause, at fixed  $\text{pH}=5$ , and according to Eqs. (2) and (3), the cationic and anionic charges were not equally distributed between the principal cationic and anionic species, that are recorded as

Table 6

Mass distribution of aqueous inorganic and organic species at  $\text{pH}=0.5$  and  $I=0.2137$  from  $10^{-3}$  M  $\text{CsNO}_3$  and 1 M acetate solution

| Component                    | Total dissolved | % dissolved | Total sorbed |
|------------------------------|-----------------|-------------|--------------|
| Acetate <sup>-1</sup>        | 1.0162E-01      | 100         | 0            |
| Cs <sup>+</sup>              | 1.0000E-03      | 100         | 0            |
| H <sup>+</sup>               | 5.2696E-01      | 100         | 0            |
| NO <sub>3</sub> <sup>-</sup> | 1.0000E-03      | 100         | 0            |

Table 7

Concentrations and activities ( $\text{mol L}^{-1}$ ) of aqueous inorganic and organic species at  $\text{pH}=0.5$  and  $I=0.2137$  from  $10^{-3}$  M  $\text{CsNO}_3$  and 1 M EDTA solution

|                                | Concentration     | Activity          | Log activity |
|--------------------------------|-------------------|-------------------|--------------|
| $\text{Cs}^+$                  | 0.000999          | 0.000774          | -3.111       |
| $\text{CsEDTA-3}$              | $1.52\text{E-}23$ | $1.53\text{E-}24$ | -23.814      |
| $\text{CsNO}_3$ (aq)           | $5.11\text{E-}07$ | $6.28\text{E-}07$ | -6.202       |
| $\text{EDTA}^{-4}$             | $1.04\text{E-}20$ | $1.76\text{E-}22$ | -21.753      |
| $\text{H}^+$                   | 0.4081            | 0.31623           | -0.5         |
| $\text{H}_2\text{EDTA}^{-2}$   | $8.14\text{E-}06$ | $2.94\text{E-}06$ | -5.532       |
| $\text{H}_3\text{EDTA}^-$      | 0.001568          | 0.001215          | -2.915       |
| $\text{H}_4\text{EDTA}$ (aq)   | 0.051125          | 0.062898          | -1.201       |
| $\text{H}_5\text{EDTA}^+$      | 0.81172           | 0.62898           | -0.201       |
| $\text{H}_6\text{EDTA}^{+2}$   | 0.42629           | 0.15369           | -0.813       |
| $\text{HEDTA}(\text{ii})^{-3}$ | $4.92\text{E-}11$ | $4.95\text{E-}12$ | -11.305      |
| $\text{NO}_3^{-1}$             | 0.000999          | 0.000774          | -3.111       |
| $\text{OH}^-$                  | $4.11\text{E-}14$ | $3.18\text{E-}14$ | -13.497      |

Table 8

Distribution of aqueous inorganic and organic species at  $\text{pH}=0.5$  and  $I=0.2137$  from  $10^{-3}$  M  $\text{CsNO}_3$  and 1 M EDTA solution

| Component          | % of total concentration | Species name                 |
|--------------------|--------------------------|------------------------------|
| $\text{EDTA}^{-4}$ | 33.028                   | $\text{H}_6\text{EDTA}^{+2}$ |
|                    | 0.121                    | $\text{H}_3\text{EDTA}^-$    |
|                    | 3.961                    | $\text{H}_4\text{EDTA}$ (aq) |
|                    | 62.889                   | $\text{H}_5\text{EDTA}^+$    |
|                    | 99.949                   | $\text{Cs}^+$                |
| $\text{Cs}^+$      | 0.051                    | $\text{CsNO}_3$ (aq)         |
|                    | 99.949                   | $\text{NO}_3^-$              |
| $\text{NO}_3^-$    | 0.051                    | $\text{CsNO}_3$ (aq)         |

$0.42634$  cation  $\text{kg}^{-1}$  and  $9.9949 \times 10^{-4}$  anion  $\text{kg}^{-1}$ , giving rise to charge difference 99.532230%. The activities of the foremost ions were  $7.4309 \times 10^{-4}$ ,  $7.4309 \times 10^{-4}$ , and  $5.782 \times 10^{-7}$  for  $\text{Cs}^+$ ,  $\text{NO}_3^-$ , and  $\text{CsNO}_3$ , respectively.

Table 9

Mass distribution of aqueous inorganic and organic species at  $\text{pH}=0.5$  and  $I=0.2137$  from  $10^{-3}$  M  $\text{CsNO}_3$  and 1 M EDTA solution

| Component          | Total dissolved | % dissolved | Total sorbed |
|--------------------|-----------------|-------------|--------------|
| $\text{Cs}^+$      | 0.001           | 100         | 0            |
| $\text{EDTA}^{-4}$ | 1.2907          | 100         | 0            |
| $\text{H}^+$       | 7.2336          | 100         | 0            |
| $\text{NO}_3^-$    | 0.001           | 100         | 0            |

Table 10

Concentrations and activities ( $\text{mol L}^{-1}$ ) of aqueous inorganic and organic species at  $\text{pH}=0.5$  and  $I=0.2137$  from  $10^{-3}$  M  $\text{CsNO}_3$  and 1 M  $\text{NaNO}_3$  solution

|                      | Concentration       | Activity            | Log activity |
|----------------------|---------------------|---------------------|--------------|
| $\text{Cs}^+$        | $1.4332\text{E-}04$ | $1.1106\text{E-}04$ | -3.954       |
| $\text{CsNO}_3$ (aq) | $8.4987\text{E-}04$ | $1.0456\text{E-}03$ | -2.981       |
| $\text{H}^+$         | $4.0810\text{E-}01$ | $3.1623\text{E-}01$ | -0.500       |
| $\text{Na}^+$        | $1.4075\text{E+}00$ | $1.0906\text{E+}00$ | 0.038        |
| $\text{NaNO}_3$ (aq) | $2.2463\text{E+}00$ | $2.7636\text{E+}00$ | 0.441        |
| $\text{NaOH}$ (aq)   | $3.5536\text{E-}14$ | $4.3719\text{E-}14$ | -13.359      |
| $\text{NO}_3^-$      | $1.1603\text{E+}01$ | $8.9909\text{E+}00$ | 0.954        |
| $\text{OH}^-$        | $4.1093\text{E-}14$ | $3.1842\text{E-}14$ | -13.497      |

Table 11

Distribution of aqueous inorganic and organic species at  $\text{pH}=0.5$  and  $I=0.2137$  from  $10^{-3}$  M  $\text{CsNO}_3$  and 1 M  $\text{NaNO}_3$  solution

| Component       | % of total concentration | Species name         |
|-----------------|--------------------------|----------------------|
| $\text{Cs}^+$   | 14.431                   | $\text{Cs}^{+1}$     |
|                 | 85.569                   | $\text{CsNO}_3$ (aq) |
| $\text{NO}_3^-$ | 83.775                   | $\text{NO}_3^{-1}$   |
|                 | 16.219                   | $\text{NaNO}_3$ (aq) |
| $\text{Na}^+$   | 38.521                   | $\text{Na}^{+1}$     |
|                 | 61.479                   | $\text{NaNO}_3$ (aq) |

Tables 1–6 show the variations present because of adding acetic acid as a complexing agent. In low acetic acid concentrations, namely,  $1 \times 10^{-8}$  M (Tables 1–3), the ionic strength and charge difference calculated were about 0.2137 and 99.532%, which could be attributed to the recorded cations and anions concentrations. The equilibrium cations were about  $4.2 \times 10^{-1}$  cation  $\text{kg}^{-1}$ , while the corresponding anions were about  $9.2 \times 10^{-1}$  that were distributed in solution as shown in Tables 1 and 2. According to Table 3, the

Table 12

Mass distribution of aqueous inorganic and organic species at  $\text{pH}=0.5$  and  $I=0.2137$  from  $10^{-3}$  M  $\text{CsNO}_3$  and 1 M  $\text{NaNO}_3$  solution

| Component       | Total dissolved     | % dissolved | Total sorbed |
|-----------------|---------------------|-------------|--------------|
| $\text{Cs}^+$   | $9.9319\text{E-}04$ | 100.000     | 0            |
| $\text{H}^+$    | $4.0810\text{E-}01$ | 100.000     | 0            |
| $\text{Na}^+$   | $3.6538\text{E+}00$ | 100.000     | 0            |
| $\text{NO}_3^-$ | $1.3850\text{E+}01$ | 100.000     | 0            |

species are neither sorbed onto the exchanger nor precipitated in solution.

On increasing the acetic acid content to 1 M, the resultant cationic, anionic concentrations, and charge difference were about  $4.2634 \times 10^{-1}$  cation  $\text{kg}^{-1}$ ,  $9.9949 \times 10^{-4}$  anion  $\text{kg}^{-1}$ , and 99.532230, respectively. As shown in Tables 4–6, increasing the acetate content led to increase in the Cs-acetate complexation from  $3.28 \times 10^{-16}$  to  $3.3293 \times 10^{-9}$ , although the acetate itself has a reversed activity when the concentration increased. This could be attributed to the increased stability constant for Cs-acetate complex in the aqueous phase with expanding the acetic acid concentration.

Tables 7–9 show the different species present in solution as a result of coexistence of cesium nitrate and EDTA whose concentrations are distributed in the following species order:  $\text{Cs}^+$ ,  $\text{CsEDTA}^{-3}$ ,  $\text{CsNO}_3$  (aq),  $\text{EDTA}^{-4}$ ,  $\text{H}^+$ ,  $\text{H}_2\text{EDTA}^{-2}$ ,  $\text{H}_3\text{EDTA}^{-}$ ,  $\text{H}_4\text{EDTA}$  (aq),  $\text{H}_5\text{EDTA}^+$ ,  $\text{H}_6\text{EDTA}^{+2}$ ,  $\text{HEDTA}(\text{ii})^{-3}$ ,  $\text{NO}_3^{-1}$ ,  $\text{OH}^-$ , as 0.000999,  $1.52 \times 10^{-23}$ ,  $5.11 \times 10^{-7}$ ,  $1.04 \times 10^{-20}$ , 0.4081,  $8.14 \times 10^{-6}$ , 0.001568, 0.051125, 0.81172, 0.42629,  $4.92 \times 10^{-11}$ , 0.000999, and  $4.11 \times 10^{-14}$ , correspondingly. In contrast to the case of acetic acid, the activity is less than the concentration in Cs-EDTA complexation. The main species present in solution were distributed according to their types. The total EDTA species,  $\text{EDTA}^{-4}$ , were distributed as  $\text{H}_6\text{EDTA}^{+2}$  (33.028%),  $\text{H}_3\text{EDTA}^{-}$  (0.121%),  $\text{H}_4\text{EDTA}$  (aq), (3.961%), and  $\text{H}_5\text{EDTA}^+$  (62.889%). On the other side, the inorganic cesium ion was found distributed as free  $\text{Cs}^+$  (99.949%) and  $\text{CsNO}_3$  (aq) (0.051%), while the nitrate anion was distributed as  $\text{NO}_3^{-}$  (99.949%) and  $\text{CsNO}_3$  (aq) (0.051%). The mass distribution of all cases showed no adsorbed species, as no adsorbent was added until this moment.

Table 13

Concentrations and activities ( $\text{mol L}^{-1}$ ) of aqueous inorganic and organic species at  $\text{pH}=0.5$  and  $I=0.2137$  from  $10^{-3}$  M  $\text{CsNO}_3$  and 1 M  $\text{NaCl}$  solution

|                      | Concentration | Activity   | Log activity |
|----------------------|---------------|------------|--------------|
| $\text{Cl}^-$        | 1.8374E+00    | 1.4238E+00 | 0.153        |
| $\text{Cs}^+$        | 1.2734E-04    | 9.8675E-05 | -4.006       |
| $\text{CsCl}$ (aq)   | 9.0708E-05    | 1.1160E-04 | -3.952       |
| $\text{CsNO}_3$ (aq) | 7.7514E-04    | 9.5363E-04 | -3.021       |
| $\text{H}^+$         | 4.0810E-01    | 3.1623E-01 | -0.500       |
| $\text{Na}^+$        | 1.1833E+00    | 9.1692E-01 | -0.038       |
| $\text{NaCl}$ (aq)   | 5.3183E-01    | 6.5429E-01 | -0.184       |
| $\text{NaNO}_3$ (aq) | 1.9387E+00    | 2.3851E+00 | 0.378        |
| $\text{NaOH}$ (aq)   | 2.9876E-14    | 3.6756E-14 | -13.435      |
| $\text{NO}_3^-$      | 1.1911E+01    | 9.2294E+00 | 0.965        |
| $\text{OH}^-$        | 4.1093E-14    | 3.1842E-14 | -13.497      |

On contrast to acetic acid and EDTA as complexing agents, sodium nitrate and sodium chloride were used as competing ions, especially when nitrate is selected as a common ion and chloride as a new counter one. The data are listed in Tables 10–15. The ionic strength was kept as 0.9000 to overcome the misleading results for activity and activity coefficients. In case of sodium nitrate addition, 1.8157 cation  $\text{kg}^{-1}$  and 11.603 anion  $\text{kg}^{-1}$  were recorded with 72.937760% charge difference percentage. However, in case of sodium chloride addition, the charge difference was about 79.249535% due to the presence of 1.5915 cation  $\text{kg}^{-1}$  and 13.748 anion  $\text{kg}^{-1}$ . Because of sodium chloride presence, the halite phase is possibly encountered with 1:1 stoichiometry mineral. The mentioned mineral was under saturation, whose saturation index could be calculated by the following equation:

$$\text{SI} = \log \left[ \frac{\text{IAP}}{K_{sp}} \right] \quad (9)$$

where  $K_{sp}$  is the solubility product that is related to the equilibrium constant, IAP is the ion activity product that is the product of free ion species activities, and SI is the saturation Index of solid phase and dissociated species in certain solubility reaction. If  $\text{IAP} > K_{sp}$ , subsequently the mineral could be precipitated. However, if  $\text{IAP} = K_{sp}$ , SI is zero and the mineral is in equilibrium with solution. In case of halite, the logarithm of ionic activity product and the corresponding saturation index were about 0.116 and -1.434, respectively.

Table 14

Distribution of aqueous inorganic and organic species at  $\text{pH}=0.5$  and  $I=0.2137$  from  $10^{-3}$  M  $\text{CsNO}_3$  and 1 M  $\text{NaCl}$  solution

| Component       | % of total concentration | Species name         |
|-----------------|--------------------------|----------------------|
| $\text{Cl}^-$   | 77.550                   | $\text{Cl}^-$        |
|                 | 22.446                   | $\text{NaCl}$ (aq)   |
| $\text{NO}_3^-$ | 85.997                   | $\text{NO}_3^-$      |
|                 | 13.997                   | $\text{NaNO}_3$ (aq) |
| $\text{Na}^+$   | 32.386                   | $\text{Na}^+$        |
|                 | 53.059                   | $\text{NaNO}_3$ (aq) |
|                 | 14.555                   | $\text{NaCl}$ (aq)   |
| $\text{Cs}^+$   | 12.822                   | $\text{Cs}^+$        |
|                 | 78.045                   | $\text{CsNO}_3$ (aq) |
|                 | 9.133                    | $\text{CsCl}$ (aq)   |

Table 15

Mass distribution of aqueous inorganic and organic species at pH=0.5 and  $I=0.2137$  from  $10^{-3}$  M CsNO<sub>3</sub> and 1 M NaCl solution

| Component                    | Total dissolved | % dissolved | Total sorbed |
|------------------------------|-----------------|-------------|--------------|
| Cl <sup>-</sup>              | 2.3693E+00      | 100.000     | 0            |
| Cs <sup>+</sup>              | 9.9319E-04      | 100.000     | 0            |
| H <sup>+</sup>               | 4.0810E-01      | 100.000     | 0            |
| Na <sup>+</sup>              | 3.6538E+00      | 100.000     | 0            |
| NO <sub>3</sub> <sup>-</sup> | 1.3850E+01      | 100.000     | 0            |

### 3.3. Traditional ion-exchange studies

#### 3.3.1. Preliminary kinetic studies

Figs. 1 and 2 show the static adsorption curves of <sup>134</sup>Cs<sup>+</sup> onto ZM and ZIM. All adsorbents had a high adsorption rate during the early period of adsorption (60 min, corresponding to the adsorption section for rotary wheel), and the adsorption reached saturation after 80 min. The saturated adsorptive ratio ( $R_s$ ) of the ZIM was superior to that of ZM under various investigated conditions. For the same adsorbent, it was found that the  $R_s$  improved with the increase in temperature. The early adsorption rate and the saturated adsorptive ratio reduced in the order of ZIM and ZM, which was consistent with diminishing BET surface area order. The prepared ZIM and ZM possessed  $175.36 \text{ m}^2 \text{ g}^{-1}$  and  $226.48 \text{ m}^2 \text{ g}^{-1}$ ,  $S_{\text{BET}}$ , respectively.

The adsorption capacity of adsorbent ( $2.33 \text{ mmol g}^{-1}$  and  $3.47 \text{ mmol g}^{-1}$ ) was closely related to its recorded surface area, the average pore size,  $D_{\text{av}}$  ( $12.36 \text{ \AA}$  and  $3.27 \text{ \AA}$ ) pore volume,  $V$  ( $0.23 \text{ cm}^3 \text{ g}^{-1}$  and  $0.524 \text{ cm}^3 \text{ g}^{-1}$ ) for ZM and ZIM, respectively. It was found that the sizable pore size and/or pore volume could reduce the diffusion resistance and hence increased the adsorption rate. Meanwhile, the large BET surface area also favored the dissipation of the adsorption heat through the solid adsorbent surface, and facilitated the adsorption process.

#### 3.3.2. Adsorption isotherm models

Some equilibrium isotherm Equations were used to describe experimental adsorption data. The equation parameters and the underlying thermodynamic assumptions of these equilibrium models often provide some insight into both the adsorption mechanism and affinity of the surface.

**3.3.2.1. The Langmuir isotherm.** In 1916, Langmuir [23] developed a theoretical equilibrium isotherm relating the amount of gas adsorbed on the surface to the

pressure of the gas. The Langmuir model is probably the best-known and most widely applied adsorption isotherm. It has produced good agreement with a wide variety of experimental data and may be represented as follows:

$$q_e = \frac{K_l X_m C_e}{1 + K_l C_e} \quad (10)$$

where  $K_l$  is Langmuir constant and  $X_m$  is maximum saturation capacity of adsorbent ( $\text{mg g}^{-1}$ ).

**3.3.2.2. The Freundlich isotherm.** In 1906, Freundlich [23] presented the earliest known adsorption isotherm equation. This empirical model can be applied to non-ideal adsorption on heterogeneous surfaces as well as multilayer adsorption, and it is formulated by the following equation:

$$q_e = k_f C_e^{1/n} \quad (11)$$

where  $K_f$  is Freundlich constant and  $n$  is a parameter.

**3.3.2.3. The Temkin isotherm.** Temkin isotherm deliberates the effects of the heat of adsorption that decreases linearly with coverage of the adsorbate and adsorbent interactions [23]. These isotherms have been reported for the adsorption of diverse anions and organic molecules onto varying substrates. This equation has generally been applied in the following form:

$$\frac{q_e}{X_m} = B_1 \ln(K_T C_e) \quad (12)$$

where  $B_1$  is Temkin parameter and  $K_T$  is Temkin constant.

**3.3.2.4. The BET isotherm.** Brunauer, Emmet, and Teller [24] developed a simple isotherm pattern (BET isotherm), which takes into account the multilayer adsorption, extracting the monolayer capacity, and hence the SSA. A number of refinements to the BET model and to the experimental method had been developed more recently, but the basic BET method remains the widely used technique for measurements of the SSA. This equation for liquid solution is:

$$q_e = X_m \frac{K_s C_e}{(1 - K_l C_e)(1 - K_l C_e + K_s C_e)} \quad (13)$$

where  $K_l$  and  $K_s$  are BET constants.

3.3.2.5. *The Sips (or Langmuir and Freundlich) isotherm.* Sips [25] derived an isotherm equation, which was valid for localized adsorption, without adsorbate–adsorbate interactions. In the low-pressure region, this equation reduces to Freundlich isotherm. The Sips equation is expressed in the following form:

$$q_e = X_m \frac{(K_l C_e)^{1/n}}{1 + (K_l C_e)^{1/n}} \quad (14)$$

where  $K_l$  and  $n$  are same as defined in Eqs. (10) and (11).

3.3.2.6. *Nonlinear regression analysis.* All the model parameters were assessed by nonlinear regression using the Graph Pad Prism 5.x software (Dennis Radashev, USA). The optimization routine required a defined error function in order to evaluate the fit of equation to the experimental data [23]. Apart from the nonlinear regression coefficient ( $R^2$ ), the sum of squared error (SSE) and the standard deviation of residuals ( $S_{yx}$ ) were used to gauge the goodness-of-fit. SSE and  $S_{yx}$  are defined as:

$$SSE = \sum_{i=1}^m (Q_i - q_i)^2 \quad (15)$$

$$S_{yx} = \sqrt{\frac{SSE}{df}} \quad (16)$$

where  $q_i$  is the observation from the experiment  $i$ ,  $Q_i$  is the estimate from the isotherm for corresponding  $q_i$ ,  $m$  is the number of observations in the experimental isotherm, and  $df$  is degree of freedom ( $df$  is the number of data points minus the number of parameters fit). The smaller values of  $S_{yx}$  and  $SSE$  indicate the better curve fitting [26].

Based on Eqs. (5)–(7), all Eqs. (10)–(16) used for expressing the adsorption equilibrium are generally represented in the form of activities instead of the usual concentrations. Figs. 3 and 4 show the different isothermal models that describe the effect of equilibrium concentration on the quantity adsorbed of  $^{134}\text{Cs}^+/\text{ZM}$  and  $^{134}\text{Cs}^+/\text{ZIM}$  at equilibrium. It could be seen from the figures and after calculation of the values of  $R^2$ ,  $SSE$ , and  $S_{yx}$  for all adsorption systems that, the Sips isotherm is the best. For the Sips equation,  $R^2$  varied from 0.9759 to 1, and this model provided a good fit to the experimental data with low  $SSE$  and  $S_{yx}$  values as compared to the other models. The obtained results showed that the best-fitted adsorption

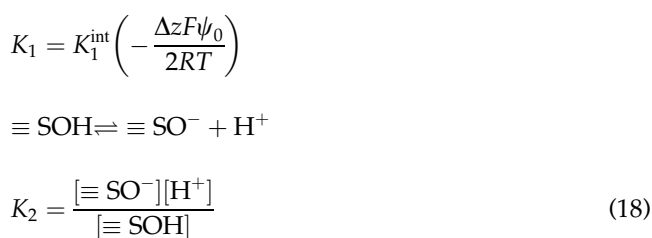
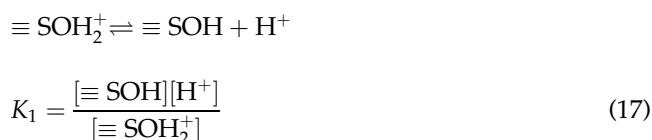
isotherm models were in the order of  $\text{BET} > \text{Freundlich} > \text{Temkin} > \text{Sips} > \text{Langmuir}$  in case of  $^{134}\text{Cs}^+/\text{ZM}$ , while the order was  $\text{Temkin} > \text{Freundlich} > \text{BET} > \text{Langmuir} > \text{Sips}$  in case of  $^{134}\text{Cs}^+/\text{ZIM}$ . The correlation coefficients of the BET in case of  $^{134}\text{Cs}^+/\text{ZM}$  and the Temkin in case of  $^{134}\text{Cs}^+/\text{ZIM}$  were about 0.999 and 9.989, respectively.

### 3.4. Establishment of Ibrahim- El-Gammal Surface Site Competition Complexation Model (SSCCM)

In this part, the new model by G. M. Ibrahim and B. El-Gammal was developed so it describes the surface site reactions for a certain cation in presence of competing and complexing ligands. Theoretical basis, postulates, and verification of the SSCCM were scientifically discussed.

#### 3.4.1. Theoretical framework of Ibrahim-El-Gammal SSCCM

The acidic–basic properties of the oxide are described in this work using a surface complexation approach with a 2-pK model by Eqs. (17), (18) with the constants  $K_1$  and  $K_2$ , respectively, defined as below.



where  $\psi_0$  is the surface potential, depending upon the model chosen to describe the interface,  $F$  is the Faraday's constant ( $96485.309 \text{ C mol}^{-1}$ ),  $R$  is the gas constant ( $8.31451 \text{ J mol}^{-1} \text{ K}^{-1}$ ),  $T$  is the absolute temperature (K), and  $\Delta z$  is the charge changing at the surface. In both Eqs. (17) and (18),  $\Delta z = -1$ . This hypothesis implies that the sites attainable by titration are amphoteric, which is not always verified [27].

The constant capacitance model (CCM) is the simplest description of the interface. In this model, acid adsorption is based on a ligand-exchange mechanism. All surface complexes are considered inner-sphere complexes and the background electrolyte ions do not form surface complexes, so that the relationship between surface charge ( $\sigma$  in  $C\ m^{-2}$ ) and surface potential ( $\psi_0$  in V) is linear [28] as

$$\sigma = C\psi_0 \quad (19)$$

where  $C$  is the capacitance ( $F\ m^{-2}$ ) of the system.

Sposito [29] explained that this model cannot be used to describe adsorption as a function of ionic strength, and that it should be restricted to specifically adsorbing ions forming inner-sphere complexes with little dependence on the ions. This model was originally restricted to high ionic strength conditions ( $I > 0.1\ mol\ L^{-1}$ ) but Lützenkirchen [30] proposed that it can be also applied to lower ionic strengths. This model requires a low number of adjustable parameters, namely the capacity  $C$ , which is ionic strength dependent, surface site concentration  $N_s$ , and the surface acidity constants  $^{int}K_1$  and  $^{int}K_2$  from reactions represented by Eqs. (17) and (18).

The double DLM [31,32] describes the interface as composed of a double layer of counter-ions at the surface to compensate surface charge of the particle. The compact layer, closely linked to the surface, and the diffuse layer, where both counter-ions and co-ions are present and the interactions between the ions and the oxide surface are weaker. The diffuse layer does not migrate with the particle. The potential at the compact/diffuse boundary (shear plane) is called  $\zeta$ -potential.

In the framework of the DLM, surface charge of an oxide in a 1:1 electrolyte is given by:

$$\sigma = \sqrt{8RT\epsilon_R\epsilon_0 I 10^3} \sinh\left(\frac{zF\psi_0}{2RT}\right) \quad (20)$$

where  $\epsilon_R$  is the relative dielectric constant of the medium (80.2 for water at 293.15 K),  $\epsilon_0$  is the vacuum dielectric constant ( $8.854 \times 10^{-12}\ C^2\ N^{-1}\ m^{-2}$ ),  $z$  is the electrolyte ion charge, and  $I$  is the ionic strength ( $mol\ L^{-1}$ ). Then, expressing  $\sigma$  as a function of the oxide parameters and site concentration leads to:

$$\sigma = \frac{F}{C_{sS}} ([\equiv SOH_2^+] - [\equiv SO^-]) \quad (21)$$

$$\sigma = \frac{F}{C_{sS}} [\equiv SOH] \left( \frac{[H^+]}{K_1^{int} \exp\left(\frac{F\psi_0}{RT}\right)} - \frac{K_2^{int} \exp\left(\frac{F\psi_0}{RT}\right)}{[H^+]} \right) \quad (22)$$

Rearranging Eqs. (20) and (22) e.g. in the case of the DLM, leads to:

$$\frac{\left( \frac{[H^+]}{K_1^{int} \exp\left(\frac{F\psi_0}{RT}\right)} - \frac{K_2^{int} \exp\left(\frac{F\psi_0}{RT}\right)}{[H^+]} \right)}{\left( \frac{1+[H^+]}{K_1^{int} \exp\left(\frac{F\psi_0}{RT}\right)} - \frac{K_2^{int} \exp\left(\frac{F\psi_0}{RT}\right)}{[H^+]} \right)} = \frac{\sqrt{8\epsilon_R\epsilon_0 RT I 10^3}}{\equiv SOH} \times \frac{C_{sS}}{F} \times \sinh\left(\frac{F\psi_0}{RT}\right) \quad (23)$$

The calculation of the  $\zeta$ -potential from  $\psi_0$  is given in [33] in the DLM framework:

$$\tanh\left(\frac{ze\zeta}{4kT}\right) = \tanh\left(\frac{ze\psi_0}{4kT}\right) \exp(\kappa x) \quad (24)$$

where  $z$  is the electrolyte ion charge,  $e$  is the elementary charge of electron ( $1.602 \times 10^{-19}\ C$ ),  $k$  the Boltzmann constant ( $1.38 \times 10^{-23}\ J\ K^{-1}$ ),  $\kappa$  ( $nm^{-1}$ ) is the reverse Debye length, and  $x$  (nm) is the distance at which  $\zeta$ -potential is measured. Some authors define that distance as the outer Helmholtz plane using the more advanced TLM ( $\zeta = \psi_d$ ), but we will adjust this parameter, as well as  $\log_{10}^{int}K_i$  values, by a trial-and-error approach to minimize the sum of squares. This definition implies that the permittivity is autonomous of position — or that the properties of water are the same whatever the distance to the surface —, which can be questioned knowing literature values [34], and recent advances on the structure of water at the surface [35].

Practically, the oxide surface charge can be determined either by potentiometric or electrophoretic titrations. The fitting of the data with an appropriate surface complexation model permits to determine the oxide characteristics. Moreover, determining the point of zero charge (PZC) of the oxide is of importance. PZC is the pH at which the surface charge of the oxide is nil. Following this, generic names are of several definitions, depending on the authors and experimental method. The evolution of electrophoretic mobility of particles as a function of pH leads to the determination of the isoelectric point (IEP), defined as the pH, where the electrophoretic mobility is nil [36]. Potentiometric titrations of the oxide performed at various ionic strengths lead to the determination of

Table 16

Ibrahim-El-Gammal SSCCM constants for sorption of  $^{134}\text{Cs}^+/\text{ZM}$  and  $^{134}\text{Cs}^+/\text{ZIM}$  in presence of different complexing agents and their verification using different statistical methods

| Equation                | $\log k_d = -K_{GB} \log[L_{\text{TOTAL}}] + \log I_{GB}$ |          |                   |          |                                |                |                   |         |
|-------------------------|---|----------|-------------------|----------|--------------------------------|----------------|-------------------|---------|
|                         | $^{134}\text{Cs}^+/\text{ZM}$                             |          |                   |          | $^{134}\text{Cs}^+/\text{ZIM}$ |                |                   |         |
| System                  |   |          |                   |          |                                |                |                   |         |
| Agent                   | CH <sub>3</sub> COOH                                      | EDTA     | NaNO <sub>3</sub> | NaCl     | CH <sub>3</sub> COOH           | EDTA           | NaNO <sub>3</sub> | NaCl    |
| Residual Sum of Squares | 0.04152   | 0.0957   | 0.0538            | 0.02145  | 0.02341                        | 0.10578        | 0.11676           | 0.04489 |
| Pearson's r             | -0.94906  | -0.95871 | -0.96698          | -0.97756 | -0.96456                       | -0.96819       | -0.92894          | -0.9424 |
| Adj. R-Square           | 0.88417   | 0.90564  | 0.92423           | 0.94822  | 0.91877                        | 0.92696        | 0.84008           | 0.8696  |
| Equation parameters     |   | Value    | Standard Error    |          | Value                          | Standard Error |                   |         |
| CH <sub>3</sub> COOH    | Log $I_{GB}$  | 2.69667  | 0.05185           |          | $I$                            | 3.1286         | 0.03893           |         |
| CH <sub>3</sub> COOH    | $K_{GB}$  | 0.08691  | 0.01178           |          | $K_{GB}$                       | 0.0792         | 0.00885           |         |
| EDTA                    | Log $I_{GB}$  | 1.96475  | 0.07872           |          | $I$                            | 2.60625        | 0.08276           |         |
| EDTA                    | $K_{GB}$  | 0.14767  | 0.01788           |          | $K_{GB}$                       | 0.17821        | 0.0188            |         |
| NaNO <sub>3</sub>       | Log $I_{GB}$  | 2.36361  | 0.05902           |          | $I$                            | 2.50316        | 0.08695           |         |
| NaNO <sub>3</sub>       | $K_{GB}$  | 0.12462  | 0.01341           |          | $K_{GB}$                       | 0.1214         | 0.01975           |         |
| NaCl                    | Log $I_{GB}$  | 2.43442  | 0.03727           |          | $I$                            | 2.66084        | 0.05391           |         |
| NaCl                    | $K_{GB}$  | 0.09622  | 0.00847           |          | $K_{GB}$                       | 0.08457        | 0.01225           |         |

Table 17

Concentrations and activities (mol L<sup>-1</sup>) of aqueous inorganic and organic species at pH=0.5 and  $I=0.2137$  from 10<sup>-3</sup> M CsNO<sub>3</sub> and 1 M acetate solution in presence of ZM as adsorbent ( $V/m = 100 \text{ mL g}^{-1}$ )

|  | Concentration | Activity | Log activity |
|--|---------------|----------|--------------|
| =SOH(1)  | 1.6E-07       | 1.6E-07  | -6.797       |
| =SOH <sub>2</sub> <sup>+</sup> (1)                           | 0.010024      | 0.010024 | -1.999       |
| Acetate <sup>-</sup>   | 8.93E-06      | 6.92E-06 | -5.16        |
| Cs <sup>+</sup>  | 0.001         | 0.000775 | -3.111       |
| Cs <sup>+</sup> D(1)   | 2.44E-19      | 2.44E-19 | -18.612      |
| Cs-Acetate (aq)  | 3.31E-09      | 4.07E-09 | -8.391       |
| CsNO <sub>3</sub> (aq)                                       | 2.33E-18      | 2.86E-18 | -17.543      |
| H <sup>+</sup>   | 0.4081        | 0.31623  | -0.5         |
| H <sup>+</sup> D(1)  | 9.98E-17      | 9.98E-17 | -16.001      |
| H <sub>2</sub> Mo <sub>6</sub> O <sub>21</sub> <sup>-4</sup> | 8,755,300     | 147,910  | 5.17         |
| H <sub>3</sub> Mo <sub>8</sub> O <sub>28</sub> <sup>-5</sup> | 1.02E+11      | 1.74E+08 | 8.24         |
| H-Acetate (aq)   | 0.10162       | 0.12502  | -0.903       |
| HMo <sub>7</sub> O <sub>24</sub> <sup>-5</sup>               | 70,661,000    | 120,230  | 5.08         |
| HMoO <sub>4</sub> <sup>-</sup>                               | 0.000709      | 0.00055  | -3.26        |
| Mo <sub>7</sub> O <sub>24</sub> <sup>-6</sup>                | 7,040.7       | 0.72444  | -0.14        |
| Mo <sub>8</sub> O <sub>26</sub> <sup>-4</sup>                | 1.42E+14      | 2.4E+12  | 12.38        |
| MoO <sub>3</sub> (H <sub>2</sub> O) <sub>3</sub> (aq)        | 1.4125        | 1.7378   | 0.24         |
| MoO <sub>4</sub> <sup>-2</sup>                               | 2.77E-07      | 1E-07    | -7           |
| NO <sub>3</sub> <sup>-</sup>                                 | 4.55E-15      | 3.53E-15 | -14.452      |
| NO <sub>3</sub> <sup>-</sup> D(1)                            | 0.001         | 0.001    | -3           |
| OH <sup>-</sup>  | 4.11E-14      | 3.18E-14 | -13.497      |
| OH <sup>-</sup> D(1)   | 0.009024      | 0.009024 | -2.045       |

the point of zero salt effect (PZSE) [37]. The titration curves are altered according to ionic strength [35–37], [38,39] and the intersection point of these curves is defined as PZSE. For pH=PZSE, the cationic and anionic exchange capacities are equal. For pure oxides, with no specific adsorption, PZSE and IEP should be equal, and they can be merged together under the name PZC.

### 3.4.2. Ibrahim-El-Gammal SSCCM postulates

The traditional SCM adopt systems, which consider a charged region at the surface of the adsorbent that can interact with the counter ions in solution at that interface. However, the new Ibrahim-El-Gammal SSCCM approach considers that interaction in presence of competing ions and/or in presence of complexing agents. Such species may be positively charged as in case of competing ions or adversely charged as in case of the ligands, which have the ability to form complexes with different stabilities with the parent ion prior to its complexation to the solid surface at the interfacial region. According to the current pH, for heterogeneous surface, the following site reactions concerning protonation or deprotonation are possible:

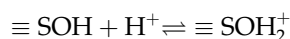


Table 18

Distribution of aqueous inorganic and organic species at pH = 0.5 and  $I = 0.2137$  from  $10^{-3}$  M CsNO<sub>3</sub> and 1 M acetate solution in presence of ZM as adsorbent ( $V/m = 100$  mL g<sup>-1</sup>)

| Component                      | % of total concentration | Species name   |
|--------------------------------|--------------------------|--|
| OH <sup>-</sup> D(1)           | 90.024                   | (1)OH <sup>-</sup> D   |
|                                | 9.976                    | (1)NO <sub>3</sub> <sup>-</sup> D                            |
| Cs <sup>+</sup>                | 100.000                  | Cs <sup>+</sup>  |
| NO <sub>3</sub> <sup>-</sup>   | 100.000                  | (1)NO <sub>3</sub> <sup>-</sup> D                            |
| Acetate <sup>-</sup>           | 99.991                   | H-Acetate (aq)   |
| H <sup>+</sup> D(1)            | 99.756                   | (1)H <sup>+</sup> D  |
|                                | 0.244                    | (1)Cs <sup>+</sup> D   |
| =SOH(1)                        | 99.998                   | =SOH <sub>2</sub> <sup>+</sup>                               |
| MoO <sub>4</sub> <sup>-2</sup> | 0.072                    | H <sub>3</sub> Mo <sub>8</sub> O <sub>28</sub> <sup>-5</sup> |
|                                | 99.928                   | Mo <sub>8</sub> O <sub>26</sub> <sup>-4</sup>                |

Table 19

Mass distribution of aqueous inorganic and organic species at pH = 0.5 and  $I = 0.2137$  from  $10^{-3}$  M CsNO<sub>3</sub> and 1 M acetate solution in presence of ZM as adsorbent ( $V/m = 100$  mL g<sup>-1</sup>)

| Component                      | Total dissolved | % dissolved | Total sorbed |
|--------------------------------|-----------------|-------------|--------------|
| =SOH(1)                        | 0               | 0.000       | 1.0024E-02   |
| Acetate <sup>-</sup>           | 1.0163E-01      | 100.000     | 0            |
| Cs <sup>+</sup>                | 1.0000E-03      | 100.000     | 2.4444E-19   |
| H <sup>+</sup>                 | 1.7051E+15      | 100.000     | 1.1024E-02   |
| MoO <sub>4</sub> <sup>-2</sup> | 1.1368E+15      | 100.000     | 0            |
| NO <sub>3</sub> <sup>-</sup>   | 4.5561E-15      | 0.000       | 1.0000E-03   |

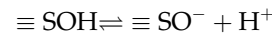
$$K_1 = \frac{[\equiv \text{SOH}_2^+]}{[\equiv \text{SOH}][\text{H}^+]} \quad (25)$$

Table 20

Formation constants and the related enthalpies of formation for inorganic and organic species at pH = 0.5 and  $I = 0.2137$  from  $10^{-3}$  M CsNO<sub>3</sub> and 1 M acetate solution in presence of ZM as adsorbent ( $V/m = 100$  mL g<sup>-1</sup>)

| Component  | log K  | $\Delta H$ (kJ mol <sup>-1</sup> ) | Stoichiometry        |                 |                |                  |                                |                              |
|--|--------|------------------------------------|----------------------|-----------------|----------------|------------------|--------------------------------|------------------------------|
|  |        |                                    | Acetate <sup>-</sup> | Cs <sup>+</sup> | H <sup>+</sup> | H <sub>2</sub> O | MoO <sub>4</sub> <sup>-2</sup> | NO <sub>3</sub> <sup>-</sup> |
| Cs-Acetate (aq)  | -0.12  | 0                                  | 1                    | 1               | 0              | 0                | 0                              | 0                            |
| CsNO <sub>3</sub> (aq)   | 0.02   | 0                                  | 0                    | 1               | 0              | 0                | 0                              | 1                            |
| H <sub>2</sub> Mo <sub>6</sub> O <sub>21</sub> <sup>-4</sup> O <sub>21</sub> <sup>-4</sup> | 51.17  | -218                               | 0                    | 0               | 8              | -3               | 6                              | 0                            |
| H <sub>3</sub> Mo <sub>8</sub> O <sub>28</sub> <sup>-5</sup>                               | 69.74  | -275                               | 0                    | 0               | 11             | -4               | 8                              | 0                            |
| H-Acetate (aq)   | 4.757  | 0.41                               | 1                    | 0               | 1              | 0                | 0                              | 0                            |
| HMo <sub>7</sub> O <sub>24</sub> <sup>-5</sup>   | 58.58  | -248                               | 0                    | 0               | 9              | -4               | 7                              | 0                            |
| HMoO <sub>4</sub> <sup>-</sup>   | 4.24   | 22                                 | 0                    | 0               | 1              | 0                | 1                              | 0                            |
| Mo <sub>7</sub> O <sub>24</sub> <sup>-6</sup>  | 52.86  | -258                               | 0                    | 0               | 8              | -4               | 7                              | 0                            |
| Mo <sub>8</sub> O <sub>26</sub> <sup>-4</sup>  | 74.38  | -285                               | 0                    | 0               | 12             | -6               | 8                              | 0                            |
| MoO <sub>3</sub> (H <sub>2</sub> O) <sub>3</sub> (aq)                                      | 8.24   | -25                                | 0                    | 0               | 2              | 0                | 1                              | 0                            |
| OH <sup>-</sup>  | -13.99 | 55.81                              | 0                    | 0               | -1             | 1                | 0                              | 0                            |

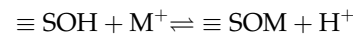
$$K_1 = K_1^{\text{int}} \left( -\frac{\Delta z F \psi_0}{2RT} \right)$$



$$K_2 = \frac{[\equiv \text{SO}^-][\text{H}^+]}{[\equiv \text{SOH}]}$$

$$K_2 = K_2^{\text{int}} \left( -\frac{\Delta z F \psi_0}{2RT} \right) \quad (26)$$

In the presence of monovalent cation, M<sup>+</sup>, a competition with the protonation reaction occurs; cation adsorption is analogous to metal hydrolysis in solution [40], so that



$$K_3 = \frac{[\equiv \text{SOM}][\text{H}^+]}{[\equiv \text{SOH}][\text{M}^+]} \quad (27)$$

$$K_3 = K_3^{\text{int}} \left( -\frac{\Delta z F \psi_0}{2RT} \right)$$

For divalent cations, M<sup>2+</sup>, the following 2 surface reactions are possible

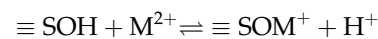


Table 21

Concentrations and activities (mol L<sup>-1</sup>) of aqueous inorganic and organic species at pH=0.5 and I=0.2137 from 10<sup>-3</sup> M CsNO<sub>3</sub> and 1 M EDTA solution in presence of ZM as adsorbent (V/m = 100 mL g<sup>-1</sup>)

|  | Concentration | Activity | Log activity |
|--|---------------|----------|--------------|
| =SOH(1)  | 1.6E-07       | 1.6E-07  | -6.797       |
| =SOH <sub>2</sub> <sup>+</sup> (1)                           | 0.010024      | 0.010024 | -1.999       |
| Cs <sup>+</sup>  | 0.001         | 0.000775 | -3.111       |
| Cs <sup>+</sup> D(1)   | 2.44E-19      | 2.44E-19 | -18.612      |
| CsEDTA <sup>-3</sup>   | 1.52E-23      | 1.53E-24 | -23.814      |
| CsNO <sub>3</sub> (aq)                                       | 2.33E-18      | 2.86E-18 | -17.543      |
| EDTA <sup>-4</sup>   | 1.04E-20      | 1.76E-22 | -21.753      |
| H <sup>+</sup>   | 0.4081        | 0.31623  | -0.5         |
| H <sup>+</sup> D(1)  | 9.98E-17      | 9.98E-17 | -16.001      |
| H <sub>2</sub> EDTA <sup>-2</sup>                            | 8.14E-06      | 2.94E-06 | -5.532       |
| H <sub>2</sub> Mo <sub>6</sub> O <sub>21</sub> <sup>-4</sup> | 8,755,300     | 147,910  | 5.17         |
| H <sub>3</sub> EDTA <sup>-</sup>                             | 0.001568      | 0.001215 | -2.915       |
| H <sub>3</sub> Mo <sub>8</sub> O <sub>28</sub> <sup>-5</sup> | 1.02E+11      | 1.74E+08 | 8.24         |
| H <sub>4</sub> EDTA (aq)                                     | 0.051125      | 0.062898 | -1.201       |
| H <sub>5</sub> EDTA <sup>+</sup>                             | 0.811172      | 0.62898  | -0.201       |
| H <sub>6</sub> EDTA <sup>+2</sup>                            | 0.42629       | 0.15369  | -0.813       |
| HEDTA(ii) <sup>-3</sup>                                      | 4.92E-11      | 4.95E-12 | -11.305      |
| HMo <sub>7</sub> O <sub>24</sub> <sup>-5</sup>               | 70,661,000    | 120,230  | 5.08         |
| HMoO <sub>4</sub> <sup>-2</sup>                              | 0.000709      | 0.00055  | -3.26        |
| Mo <sub>7</sub> O <sub>24</sub> <sup>-6</sup>                | 7,040.7       | 0.72444  | -0.14        |
| Mo <sub>8</sub> O <sub>26</sub> <sup>-4</sup>                | 1.42E+14      | 2.4E+12  | 12.38        |
| MoO <sub>3</sub> (H <sub>2</sub> O) <sub>3</sub> (aq)        | 1.4125        | 1.7378   | 0.24         |
| MoO <sub>4</sub> <sup>-2</sup>                               | 2.77E-07      | 1E-07    | -7           |
| NO <sub>3</sub> <sup>-</sup>                                 | 4.55E-15      | 3.53E-15 | -14.452      |
| NO <sub>3</sub> <sup>-</sup> D(1)                            | 0.001         | 0.001    | -3           |
| OH <sup>-</sup>  | 4.11E-14      | 3.18E-14 | -13.497      |
| OH <sup>-</sup> D(1)   | 0.009024      | 0.009024 | -2.045       |

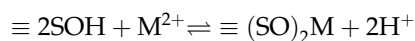
Table 22

Distribution of aqueous inorganic and organic species at pH = 0.5 and I = 0.2137 from 10<sup>-3</sup> M CsNO<sub>3</sub> and 1 M EDTA solution in presence of ZM as adsorbent (V/m = 100 mL g<sup>-1</sup>)

| Component                      | % of total concentration | Species name   |
|--------------------------------|--------------------------|--|
| OH <sup>-</sup> D(1)           | 90.024                   | (1)OH <sup>-</sup> D   |
|                                | 9.976                    | (1)NO <sub>3</sub> <sup>-</sup> D                            |
| Cs <sup>+</sup>                | 100                      | Cs <sup>+</sup>  |
| NO <sub>3</sub> <sup>-</sup>   | 100                      | (1)NO <sub>3</sub> <sup>-</sup> D                            |
| EDTA <sup>-4</sup>             | 0.121                    | H <sub>3</sub> EDTA <sup>-</sup>                             |
|                                | 3.961                    | H <sub>4</sub> EDTA (aq)                                     |
|                                | 62.889                   | H <sub>5</sub> EDTA <sup>+</sup>                             |
|                                | 33.028                   | H <sub>6</sub> EDTA <sup>+2</sup>                            |
| H <sup>+</sup> D(1)            | 99.756                   | (1)H <sup>+</sup> D  |
|                                | 0.244                    | (1)Cs <sup>+</sup> D   |
| =SOH(1)                        | 99.998                   | =SOH <sub>2</sub> <sup>+</sup>                               |
| MoO <sub>4</sub> <sup>-2</sup> | 0.072                    | H <sub>3</sub> Mo <sub>8</sub> O <sub>28</sub> <sup>-5</sup> |
|                                | 99.928                   | Mo <sub>8</sub> O <sub>26</sub> <sup>-4</sup>                |

$$K_4 = \frac{[\equiv \text{SOM}^+][\text{H}^+]}{[\equiv \text{SOH}][\text{M}^{2+}]} \quad (28)$$

$$K_4 = K_4^{\text{int}} \left( -\frac{\Delta z F \psi_0}{2RT} \right)$$



$$K_5 = \frac{[\equiv (\text{SO})_2\text{M}][\text{H}^+]^2}{[\equiv \text{SOH}]^2[\text{M}^{2+}]} \quad (29)$$

$$K_5 = K_5^{\text{int}} \left( -\frac{\Delta z F \psi_0}{2RT} \right)$$

In the presence of some competing ion and/or some complexing agents such as EDTA, the surface reaction constants are expected to decrease, due to ligand-cation complexation, or due to cation-cation completion. In other words, based on the diffuse double layer model, the novel linear relationship, the SSCCM governing the effect of ligand concentration on the sorption process on a heterogeneous surface rather than the tested isotherms could be represented as:

$$\begin{aligned} \log K_c &= -K_{GB} \log[L_{\text{TOTAL}}] + \log I_{GB} K_c \\ &= K_c^{\text{int}} \left( -\frac{\Delta z F \psi_0}{2RT} \right) \log k_d \\ &= -K_{GB} \log[L_{\text{TOTAL}}] + \log I_{GB} k_d = k_d^{\text{int}} \left( -\frac{\Delta z F \psi_0}{2RT} \right) \end{aligned} \quad (30)$$

where  $K_{GB}$  and  $I_{GB}$  are Ibrahim-El-Gammal constants, which represent the competition-complexation stability constant and the theoretical initial distribution coefficient in the absence of the complexing agent

Table 23

Mass distribution of aqueous inorganic and organic species at pH=0.5 and I=0.2137 from 10<sup>-3</sup> M CsNO<sub>3</sub> and 1 M EDTA solution in presence of ZM as adsorbent (V/m = 100 mL g<sup>-1</sup>)

| Component                      | Total dissolved | % dissolved | Total sorbed |
|--------------------------------|-----------------|-------------|--------------|
| =SOH(1)                        | 0               | 0           | 0.010024     |
| Cs <sup>+</sup>                | 0.001           | 100         | 2.44E-19     |
| EDTA <sup>-4</sup>             | 1.2907          | 100         | 0            |
| H <sup>+</sup>                 | 1.71E+15        | 100         | 0.011024     |
| MoO <sub>4</sub> <sup>-2</sup> | 1.14E+15        | 100         | 0            |
| NO <sub>3</sub> <sup>-</sup>   | 4.56E-15        | 0           | 0.001        |

Table 24

Formation constants and the related enthalpies of formation for inorganic and organic species at pH = 0.5 and  $I = 0.2137$  from  $10^{-3}$  M CsNO<sub>3</sub> and 1 M EDTA solution in presence of ZM as adsorbent ( $V/m = 100$  mL g<sup>-1</sup>)

| Component  | log K   | $\Delta H$ (kJ mol <sup>-1</sup> ) | Stoichiometry   |                    |                |                  |                                |                              |
|--|---------|------------------------------------|-----------------|--------------------|----------------|------------------|--------------------------------|------------------------------|
|  |         |                                    | Cs <sup>+</sup> | EDTA <sup>-4</sup> | H <sup>+</sup> | H <sub>2</sub> O | MoO <sub>4</sub> <sup>-2</sup> | NO <sub>3</sub> <sup>-</sup> |
| CsEDTA <sup>-3</sup>   | 1.05    | 0                                  | 1               | 1                  | 0              | 0                | 0                              | 0                            |
| CsNO <sub>3</sub> (aq)                                       | .02     | 0                                  | 1               | 0                  | 0              | 0                | 0                              | 1                            |
| H <sub>2</sub> EDTA <sup>-2</sup>                            | 17.221  | -36                                | 0               | 1                  | 2              | 0                | 0                              | 0                            |
| H <sub>2</sub> Mo <sub>6</sub> O <sub>21</sub> <sup>-4</sup> | 51.17   | -218                               | 0               | 0                  | 8              | -3               | 6                              | 0                            |
| H <sub>3</sub> EDTA <sup>-</sup>                             | 20.338  | -28.9                              | 0               | 1                  | 3              | 0                | 0                              | 0                            |
| H <sub>3</sub> Mo <sub>8</sub> O <sub>28</sub> <sup>-5</sup> | 69.74   | -275                               | 0               | 0                  | 11             | -4               | 8                              | 0                            |
| H <sub>4</sub> EDTA (aq)                                     | 22.552  | -27.9                              | 0               | 1                  | 4              | 0                | 0                              | 0                            |
| H <sub>5</sub> EDTA <sup>+</sup>                             | 24.052  | -25.9                              | 0               | 1                  | 5              | 0                | 0                              | 0                            |
| H <sub>6</sub> EDTA <sup>+2</sup>                            | 23.94   | -25.1                              | 0               | 1                  | 6              | 0                | 0                              | 0                            |
| HEDTA(ii) <sup>-3</sup>                                      | 10.948  | -21                                | 0               | 1                  | 1              | 0                | 0                              | 0                            |
| HMo <sub>7</sub> O <sub>24</sub> <sup>-5</sup>               | 58.58   | -248                               | 0               | 0                  | 9              | -4               | 7                              | 0                            |
| HMoO <sub>4</sub> <sup>-</sup>                               | 4.24    | 22                                 | 0               | 0                  | 1              | 0                | 1                              | 0                            |
| Mo <sub>7</sub> O <sub>24</sub> <sup>-6</sup>                | 52.86   | -258                               | 0               | 0                  | 8              | -4               | 7                              | 0                            |
| Mo <sub>8</sub> O <sub>26</sub> <sup>-4</sup>                | 74.38   | -285                               | 0               | 0                  | 12             | -6               | 8                              | 0                            |
| MoO <sub>3</sub> (H <sub>2</sub> O) <sub>3</sub> (aq)        | 8.24    | -25                                | 0               | 0                  | 2              | 0                | 1                              | 0                            |
| OH <sup>-</sup>  | -13.997 | 55.81                              | 0               | 0                  | -1             | 1                | 0                              | 0                            |

Table 25

Concentrations and activities (mol L<sup>-1</sup>) of aqueous inorganic and organic species at pH = 0.5 and  $I = 0.2137$  from  $10^{-3}$  M CsNO<sub>3</sub> and 1 M NaCl solution in presence of ZM as adsorbent ( $V/m = 100$  mL g<sup>-1</sup>)

|  | Concentration | Activity   | Log activity |
|--|---------------|------------|--------------|
| =SOH(1)  | 1.5967E-07    | 1.5967E-07 | -6.797       |
| =SOH <sub>2</sub> <sup>+</sup> (1)                           | 1.0024E-02    | 1.0024E-02 | -1.999       |
| Cl <sup>-</sup>  | 1.8362E+00    | 1.4228E+00 | 0.153        |
| Cl <sup>-</sup> D(1)   | 1.3397E-03    | 1.3397E-03 | -2.873       |
| Cs <sup>+</sup>  | 1.2742E-04    | 9.8734E-05 | -4.006       |
| Cs <sup>+</sup> D(1)   | 8.0033E-21    | 8.0033E-21 | -20.097      |
| CsCl (aq)  | 9.0702E-05    | 1.1159E-04 | -3.952       |
| CsNO <sub>3</sub> (aq)                                       | 7.7507E-04    | 9.5354E-04 | -3.021       |
| H <sup>+</sup>   | 4.0810E-01    | 3.1623E-01 | -0.500       |
| H <sup>+</sup> D(1)  | 2.5633E-17    | 2.5633E-17 | -16.591      |
| H <sub>2</sub> Mo <sub>6</sub> O <sub>21</sub> <sup>-4</sup> | 8.7553E+06    | 1.4791E+05 | 5.170        |
| H <sub>3</sub> Mo <sub>8</sub> O <sub>28</sub> <sup>-5</sup> | 1.0214E+11    | 1.7378E+08 | 8.240        |
| HMo <sub>7</sub> O <sub>24</sub> <sup>-5</sup>               | 7.0661E+07    | 1.2023E+05 | 5.080        |
| HMoO <sub>4</sub> <sup>-</sup>                               | 7.0920E-04    | 5.4954E-04 | -3.260       |
| Mo <sub>7</sub> O <sub>24</sub> <sup>-6</sup>                | 7.0407E+03    | 7.2444E-01 | -0.140       |
| Mo <sub>8</sub> O <sub>26</sub> <sup>-4</sup>                | 1.4199E+14    | 2.3988E+12 | 12.380       |
| MoO <sub>3</sub> (H <sub>2</sub> O) <sub>3</sub> (aq)        | 1.4125E+00    | 1.7378E+00 | 0.240        |
| MoO <sub>4</sub> <sup>-2</sup>                               | 2.7738E-07    | 1.0000E-07 | -7.000       |
| Na <sup>+</sup>  | 1.1839E+00    | 9.1734E-01 | -0.037       |
| Na <sup>+</sup> D(1)   | 7.4359E-17    | 7.4359E-17 | -16.129      |
| NaCl (aq)  | 5.3172E-01    | 6.5416E-01 | -0.184       |
| NaNO <sub>3</sub> (aq)                                       | 1.9382E+00    | 2.3845E+00 | 0.377        |
| NaOH (aq)  | 2.9890E-14    | 3.6773E-14 | -13.434      |
| NO <sub>3</sub> <sup>-</sup>                                 | 1.1903E+01    | 9.2230E+00 | 0.965        |
| NO <sub>3</sub> <sup>-</sup> D(1)                            | 8.6842E-03    | 8.6842E-03 | -2.061       |
| OH <sup>-</sup>  | 4.1093E-14    | 3.1842E-14 | -13.497      |
| OH <sup>-</sup> D(1)   | 2.9982E-17    | 2.9982E-17 | -16.523      |

Table 26

Distribution of aqueous inorganic and organic species at pH = 0.5 and  $I = 0.2137$  from  $10^{-3}$  M CsNO<sub>3</sub> and 1 M NaCl solution in presence of ZM as adsorbent ( $V/m = 100$  mL g<sup>-1</sup>)

| Component                      | % of total concentration | Species name   |
|--------------------------------|--------------------------|--|
| OH <sup>-</sup> D(1)           | 86.635                   | (1)NO <sub>3</sub> <sup>-1</sup> D                           |
|                                | 13.365                   | (1)Cl-1D   |
| NO <sub>3</sub> <sup>-</sup>   | 85.938                   | NO <sub>3</sub> <sup>-1</sup>                                |
|                                | 0.063                    | (1)NO <sub>3</sub> <sup>-</sup> D                            |
| Na <sup>+</sup>                | 13.994                   | NaNO <sub>3</sub> (aq)                                       |
|                                | 32.401                   | Na <sup>+</sup>  |
|                                | 14.552                   | NaCl (aq)  |
|                                | 53.047                   | NaNO <sub>3</sub> (aq)                                       |
| Cs <sup>+</sup>                | 12.829                   | Cs <sup>+</sup>  |
|                                | 9.132                    | CsCl (aq)  |
|                                | 78.038                   | CsNO <sub>3</sub> (aq)                                       |
| H <sup>+</sup> D(1)            | 25.633                   | (1)H <sup>+</sup> D  |
|                                | 74.359                   | (1)Na <sup>+</sup> D   |
| Cl <sup>-</sup>                | 77.498                   | Cl <sup>-</sup>  |
|                                | 22.442                   | NaCl (aq)  |
| =SOH(1)                        | 0.057                    | (1)ClD   |
|                                | 99.998                   | =SOH <sub>2</sub> <sup>+</sup>                               |
| MoO <sub>4</sub> <sup>-2</sup> | 0.072                    | H <sub>3</sub> Mo <sub>8</sub> O <sub>28</sub> <sup>-5</sup> |
|                                | 99.928                   | Mo <sub>8</sub> O <sub>26</sub> <sup>-4</sup>                |

and  $[L_{TOTAL}]$  is the total ligand concentration,  $K_c$  is the equilibrium constant, and  $k_d$  is the distribution coefficient in mL g<sup>-1</sup>. The negative sign indicates decreasing partition coefficient with increasing the ligand concentration. The SSCCM is an advantage, because it requires relatively few fit parameters and a large widespread database, as it is based on the surface site reactions [41]. However, it is expected that the stability constants are ionic-strength-independent. The SSCCM could be applied to evaluate the complex formation ability in presence of mixed ligands. By plotting a relationship between both logarithms of the equilibrium constant or the distribution

coefficient in mL g<sup>-1</sup> with the total ligand molar concentration, a straight line is expected to appear. Fitting the extrapolated straight line could fairly assess the competition-complexation stability constant and the distribution coefficient at zero-ligand concentration.

### 3.4.3. Verification of SSCCM

Based on Eq. (30), the two-layer surface site competition-complexation model incorporated into MINEQL+, v. 4.6 [42] was utilized to model <sup>134</sup>Cs<sup>+</sup>/ZM. The results of the batch experiments were compared to that obtained by MINEQL+. The two-layer SSCCM and the database of Dzombak and Morel [43] were utilized to predict <sup>134</sup>Cs<sup>+</sup> removal by ZM and ZIM with large ionic strengths. MINEQL+ utilizes the Davis equation to calculate the activity coefficients for various components. The Davis equation works well for ionic strength values less than 0.5 M, and usually, Pitzer equations are recommended to calculate the activity coefficients in high ionic strength solutions [44]. However, it is possible to use the conventional extended Debye-Huckel equation, which is similar to Davis's equation to model ion-interactions in the <sup>134</sup>Cs<sup>+</sup>/ZM and <sup>134</sup>Cs<sup>+</sup>/ZIM systems. As it could be seen from Figs. 5 and 6, the logarithmic plots of partition coefficients linearly decreased with the corresponding logarithmic equilibrium concentrations.

As shown in Table 16, the new model succeeded in explanation of the effect of ligand concentration on the partition coefficient of the original ion <sup>134</sup>Cs<sup>+</sup>/ZM and <sup>134</sup>Cs<sup>+</sup>/ZIM systems. The statistical errors are within the accepted values. In addition, the correlation coefficients could be theoretically verified. As the slope of the curve increases, the formation constant of the ion-ligand increases. In case of NaNO<sub>3</sub> and NaCl, increasing their concentration would be responsible for the same effect observed

Table 27

Saturation indices and their stoichiometries of inorganic species at pH = 0.5 and  $I = 0.2137$  from  $10^{-3}$  M CsNO<sub>3</sub> and 1 M NaCl solution in presence of ZM as adsorbent ( $V/m = 100$  mL g<sup>-1</sup>)

| Component  | logIAP  | SI     | Stoichiometry |                                |   |                 |    |                  |   |                |
|--|---------|--------|---------------|--------------------------------|---|-----------------|----|------------------|---|----------------|
| H <sub>2</sub> MoO <sub>4</sub> (s)                    | -8.000  | 4.876  | 1             | MoO <sub>4</sub> <sup>-2</sup> | 2 | H <sup>+</sup>  |    |                  |   |                |
| Halite   | 0.116   | -1.434 | 1             | Na <sup>+</sup>                | 1 | Cl <sup>-</sup> | -1 | H <sub>2</sub> O |   |                |
| MoO <sub>3</sub> (s)                                   | -8.000  | 0.000  | 1             | MoO <sub>4</sub> <sup>-2</sup> | 2 | H <sup>+</sup>  | -1 | H <sub>2</sub> O |   |                |
| Na <sub>2</sub> Mo <sub>2</sub> O <sub>7</sub> (s)     | -15.075 | 1.522  | 2             | MoO <sub>4</sub> <sup>-2</sup> | 2 | Na <sup>+</sup> | -1 | H <sub>2</sub> O | 2 | H <sup>+</sup> |
| Na <sub>2</sub> MoO <sub>4</sub> (s)                   | -7.075  | -8.565 | 1             | MoO <sub>4</sub> <sup>-2</sup> | 2 | Na <sup>+</sup> |    |                  |   |                |
| Na <sub>2</sub> MoO <sub>4</sub> ·2H <sub>2</sub> O(s) | -7.075  | -8.299 | 1             | MoO <sub>4</sub> <sup>-2</sup> | 2 | Na <sup>+</sup> | 2  | H <sub>2</sub> O |   |                |

Table 28

Mass distribution of aqueous inorganic and organic species at pH=0.5 and  $I=0.2137$  from  $10^{-3}$  M CsNO<sub>3</sub> and 1 M NaCl solution in presence of ZM as adsorbent ( $V/m=100$  mL g<sup>-1</sup>)

| Component                      | Total dissolved | % dissolved | Total sorbed |
|--------------------------------|-----------------|-------------|--------------|
| =SOH(1)                        | 0               | 0.000       | 1.0024E-02   |
| Cl <sup>-</sup>                | 2.3680E+00      | 99.943      | 1.3397E-03   |
| Cs <sup>+</sup>                | 9.9319E-04      | 100.000     | 8.0033E-21   |
| H <sub>+</sub>                 | 1.7051E+15      | 100.000     | 2.0048E-02   |
| MoO <sub>4</sub> <sup>-2</sup> | 1.1368E+15      | 100.000     | 0            |
| Na <sup>+</sup>                | 3.6538E+00      | 100.000     | 7.4359E-17   |
| NO <sub>3</sub> <sup>-</sup>   | 1.3842E+01      | 99.937      | 8.6842E-03   |

in case of acetic acid or EDTA as complexing agents. This could be attributed to completion of Na<sup>+</sup> ion with <sup>134</sup>Cs<sup>+</sup>/ZM or <sup>134</sup>Cs<sup>+</sup>/ZIM, regardless of the co-anions present in solution.

As it could be seen from the postulates, the SSCCM is ionic strength dependent. Therefore, one goal of this study is to determine whether the SSCCM can adequately describe <sup>134</sup>Cs<sup>+</sup> adsorption on ZM over significant ranges of ionic strength and sorbate/sorbent ratio as well as the mineral-mineral interactions' possibilities. ZIM was excluded from calculations due to complexity, as extra iodate surface is present. Tables 17–20 show the effect of addition of ZM as an adsorbent to the current system using  $V/m=100$  mL g<sup>-1</sup>. At the interfacial region, the sum of the cations was about

0.4091 cation kg<sup>-1</sup> and  $5.6849 \times 10^{14}$  anion kg<sup>-1</sup>, reaching a charge difference as 100%. The surface potential because of different charges distribution over the distinct planes was calculated. 1.1844E-01 V at  $\psi$  (O) plane was only present, while zero voltage were observed at (B) and (D) planes. On the other hand, the charge density,  $\sigma$ , is about 0.55267 C m<sup>-2</sup> as  $\sigma$  (O) plane, which was completely reversed, -0.55267 as  $\sigma$  (DDL) plane. Due to the addition of ZM, two species that may undergo solubility are present in the tested DL. H<sub>2</sub>MoO<sub>4</sub>(s), which has a logarithmic ionic activity product, equal to -8.000 that was precipitated as its saturation index is about 4.876. The stoichiometry of that compound is about 1, 2, and -1 for MoO<sub>4</sub><sup>-2</sup>, H<sup>+</sup> and H<sub>2</sub>O, respectively. The latter compound is MoO<sub>3</sub> (s) with a logarithmic ionic activity product equal to -8.000 which is in equilibrium between the solid and aqueous phases as its saturation index is zero.

The replacement of acetic acid with EDTA led to a change in the surface charges, on the surface, to be 2.07 cation kg<sup>-1</sup> and  $5.68 \times 10^{14}$  anion kg<sup>-1</sup> with charge difference 100%, while the same charge density held constant at 0.11856 V surface potential. As it could be seen from Tables 21–24, most of the cesium was not sorbed on the surface as it was complexed by EDTA. This result was augmented by the SSCCM stability constant and supported by the lowering  $k_d$  values with the concentration of the EDTA concentration.

On the other hand, Tables 25–34 were explained using SSCCM according to the postulate that competing ions could reduce the cation adsorption on the

Table 29

Formation constants and the related enthalpies of formation for inorganic and organic species at pH=0.5 and  $I=0.2137$  from  $10^{-3}$  M CsNO<sub>3</sub> and 1 M NaCl solution in presence of ZM as adsorbent ( $V/m=100$  mL g<sup>-1</sup>)

| Component  | log K   | $\Delta H$ (kJ mol <sup>-1</sup> ) | Stoichiometry   |                 |                |                  |                                |                                   |                 |
|--|---------|------------------------------------|-----------------|-----------------|----------------|------------------|--------------------------------|-----------------------------------|-----------------|
|  |         |                                    | Cl <sup>-</sup> | Cs <sup>+</sup> | H <sup>+</sup> | H <sub>2</sub> O | MoO <sub>4</sub> <sup>-2</sup> | N (NO <sub>3</sub> <sup>-</sup> ) | Na <sup>+</sup> |
| CsCl (aq)  | -0.1    | 0                                  | 1               | 1               | 0              | 0                | 0                              | 0                                 | 0               |
| CsNO <sub>3</sub> (aq)                                       | 0.02    | 0                                  | 0               | 1               | 0              | 0                | 0                              | 1                                 | 0               |
| H <sub>2</sub> Mo <sub>6</sub> O <sub>21</sub> <sup>-4</sup> | 51.17   | -218                               | 0               | 0               | 8              | -3               | 6                              | 0                                 | 0               |
| H <sub>3</sub> Mo <sub>8</sub> O <sub>28</sub> <sup>-5</sup> | 69.74   | -275                               | 0               | 0               | 11             | -4               | 8                              | 0                                 | 0               |
| HMo <sub>7</sub> O <sub>24</sub> <sup>-5</sup>               | 58.58   | -248                               | 0               | 0               | 9              | -4               | 7                              | 0                                 | 0               |
| HMoO <sub>4</sub>  | 4.24    | 22                                 | 0               | 0               | 1              | 0                | 1                              | 0                                 | 0               |
| Mo <sub>7</sub> O <sub>24</sub> <sup>-6</sup>                | 52.86   | -258                               | 0               | 0               | 8              | -4               | 7                              | 0                                 | 0               |
| Mo <sub>8</sub> O <sub>26</sub> <sup>-4</sup>                | 74.38   | -285                               | 0               | 0               | 12             | -6               | 8                              | 0                                 | 0               |
| MoO <sub>3</sub> (H <sub>2</sub> O) <sub>3</sub> (aq)        | 8.24    | -25                                | 0               | 0               | 2              | 0                | 1                              | 0                                 | 0               |
| NaCl (aq)  | -3      | -8                                 | 1               | 0               | 0              | 0                | 0                              | 0                                 | 1               |
| NaNO <sub>3</sub> (aq)                                       | -55     | 0                                  | 0               | 0               | 0              | 0                | 0                              | 1                                 | 1               |
| NaOH (aq)  | -13.897 | 59.81                              | 0               | 0               | -1             | 1                | 0                              | 0                                 | 1               |
| OH <sup>-</sup>  | -13.997 | 55.81                              | 0               | 0               | -1             | 1                | 0                              | 0                                 | 0               |

Table 30

Concentrations and activities ( $\text{mol L}^{-1}$ ) of aqueous inorganic and organic species at  $\text{pH}=0.5$  and  $I=0.2137$  from  $10^{-3}$  M  $\text{CsNO}_3$  and 1 M  $\text{NaNO}_3$  solution in presence of ZM as adsorbent ( $V/m = 100 \text{ mL g}^{-1}$ )

| Component  | Concentration | Activity   | Log activity |
|--|---------------|------------|--------------|
| =SOH(1)  | 1.5967E-07    | 1.5967E-07 | -6.797       |
| =SOH <sub>2</sub> <sup>+</sup> (1)                           | 1.0024E-02    | 1.0024E-02 | -1.999       |
| Cs <sup>+</sup>  | 1.4342E-04    | 1.1113E-04 | -3.954       |
| Cs <sup>+</sup> D(1)   | 7.8959E-21    | 7.8959E-21 | -20.103      |
| CsNO <sub>3</sub> (aq)                                       | 8.4977E-04    | 1.0454E-03 | -2.981       |
| H <sup>+</sup>   | 4.0810E-01    | 3.1623E-01 | -0.500       |
| H <sup>+</sup> D(1)  | 2.2468E-17    | 2.2468E-17 | -16.648      |
| H <sub>2</sub> Mo <sub>6</sub> O <sub>21</sub> <sup>-4</sup> | 8.7553E+06    | 1.4791E+05 | 5.170        |
| H <sub>3</sub> Mo <sub>8</sub> O <sub>28</sub> <sup>-5</sup> | 1.0214E+11    | 1.7378E+08 | 8.240        |
| HMo <sub>7</sub> O <sub>24</sub> <sup>-5</sup>               | 7.0661E+07    | 1.2023E+05 | 5.080        |
| HMoO <sub>4</sub> <sup>-</sup>                               | 7.0920E-04    | 5.4954E-04 | -3.260       |
| Mo <sub>7</sub> O <sub>24</sub> <sup>-6</sup>                | 7.0407E+03    | 7.2444E-01 | -0.140       |
| Mo <sub>8</sub> O <sub>26</sub> <sup>-4</sup>                | 1.4199E+14    | 2.3988E+12 | 12.380       |
| MoO <sub>3</sub> (H <sub>2</sub> O) <sub>3</sub> (aq)        | 1.4125E+00    | 1.7378E+00 | 0.240        |
| MoO <sub>4</sub> <sup>-2</sup>                               | 2.7738E-07    | 1.0000E-07 | -7.000       |
| Na <sup>+</sup>  | 1.4082E+00    | 1.0911E+00 | 0.038        |
| Na <sup>+</sup> D(1)   | 7.7525E-17    | 7.7525E-17 | -16.111      |
| NaNO <sub>3</sub> (aq)                                       | 2.2456E+00    | 2.7627E+00 | 0.441        |
| NaOH (aq)  | 3.5554E-14    | 4.3741E-14 | -13.359      |
| NO <sub>3</sub> <sup>-</sup>                                 | 1.1594E+01    | 8.9837E+00 | 0.953        |
| NO <sub>3</sub> <sup>+</sup> D(1)                            | 1.0024E-02    | 1.0024E-02 | -1.999       |
| OH <sup>-</sup>  | 4.1093E-14    | 3.1842E-14 | -13.497      |
| OH <sup>-</sup> D(1)   | 3.5529E-17    | 3.5529E-17 | -16.449      |

surface sites due to competing effect caused by the extra positively charged cation rather the steric hindrance encountered in complexation by acetic acid or

Table 31

Distribution of aqueous inorganic and organic species at  $\text{pH}=0.5$  and  $I=0.2137$  from  $10^{-3}$  M  $\text{CsNO}_3$  and 1 M  $\text{NaNO}_3$  solution in presence of ZM as adsorbent ( $V/m = 100 \text{ mL g}^{-1}$ )

| Component                      | % of total concentration | Species name   |
|--------------------------------|--------------------------|--|
| OH <sup>-</sup> D(1)           | 100.000                  | (1)NO <sub>3</sub> <sup>-</sup> D                            |
| NO <sub>3</sub> <sup>-1</sup>  | 83.708                   | NO <sub>3</sub> <sup>-</sup>                                 |
|                                | 0.072                    | (1)NO <sub>3</sub> <sup>-1</sup> D                           |
|                                | 16.214                   | NaNO <sub>3</sub> (aq)                                       |
| Na <sup>+1</sup>               | 38.540                   | Na <sub>+</sub>  |
|                                | 61.460                   | NaNO <sub>3</sub> (aq)                                       |
| Cs <sup>+1</sup>               | 14.440                   | Cs <sub>+</sub>  |
|                                | 85.560                   | CsNO <sub>3</sub> (aq)                                       |
| H <sup>+1</sup> D(1)           | 22.468                   | (1)H <sup>+</sup> D  |
|                                | 77.525                   | (1)Na <sup>+</sup> D   |
| =SOH(1)                        | 99.998                   | =SOH <sub>2</sub> <sup>+</sup>                               |
| MoO <sub>4</sub> <sup>-2</sup> | 0.072                    | H <sub>3</sub> Mo <sub>8</sub> O <sub>28</sub> <sup>-5</sup> |
|                                | 99.928                   | Mo <sub>8</sub> O <sub>26</sub> <sup>-4</sup>                |

EDTA. Moreover, increasing the ionic strengths by the addition of NaCl or NaNO<sub>3</sub> would negatively affect the sorption process by lowering the pH of the system. In <sup>134</sup>Cs<sup>+</sup>/ZM system, the charges on the molybdate surface were about 1.59 cation  $\text{kg}^{-1}$  and  $5.68 \times 10^{14}$  anion  $\text{kg}^{-1}$ , respectively. On comparing the effect of acetic acid and EDTA as complexing agents, NaCl, and NaNO<sub>3</sub> as competing media, it was found that both cases would cause lowering of the sorption content as could be explained based on the SSCCM. However, the decrease in the sorption process in the former case would be expected to be less than the later one. This could be explained by the nature of the molybdate surface, which acts as perfect cation exchanger, as well as the size of the ions resulting from the complexation process. This would result in more steric effects that can render the inner-sphere sorption or diffusion [15]. Another main difference is the formation of new solid species with different solubilities. In case of addition of NaCl to the <sup>134</sup>Cs<sup>+</sup>/ZM system, each of the subsequent species with their logarithmic ionic activity products and the corresponding saturation indices were respectively found, (H<sub>2</sub>MoO<sub>4</sub>(s), -8.000, 4.876), (Halite, 0.116, -1.434),

Table 32

Saturation indices and their stoichiometries of inorganic species at pH=0.5 and  $I=0.2137$  from  $10^{-3}$  M CsNO<sub>3</sub> and 1 M NaNO<sub>3</sub> solution in presence of ZM as adsorbent ( $V/m = 100$  mL g<sup>-1</sup>)

| Component  | logIAP  | SI     | Stoichiometry |                                |   |                 |    |                  |   |                |
|--|---------|--------|---------------|--------------------------------|---|-----------------|----|------------------|---|----------------|
| H <sub>2</sub> MoO <sub>4</sub> (s)                    | -8.000  | 4.876  | 1             | MoO <sub>4</sub> <sup>-2</sup> | 2 | H <sup>+</sup>  | -1 | H <sub>2</sub> O |   |                |
| MoO <sub>3</sub> (s)                                   | -8.000  | 0.000  | 1             | MoO <sub>4</sub> <sup>-2</sup> | 2 | H <sup>+</sup>  | -1 | H <sub>2</sub> O |   |                |
| Na <sub>2</sub> Mo <sub>2</sub> O <sub>7</sub> (s)     | -14.924 | 1.672  | 2             | MoO <sub>4</sub> <sup>-2</sup> | 2 | Na <sup>+</sup> | -1 | H <sub>2</sub> O | 2 | H <sup>+</sup> |
| Na <sub>2</sub> MoO <sub>4</sub> (s)                   | -6.924  | -8.414 | 1             | MoO <sub>4</sub> <sup>-2</sup> | 2 | Na <sup>+</sup> |    |                  |   |                |
| Na <sub>2</sub> MoO <sub>4</sub> ·2H <sub>2</sub> O(s) | -6.924  | -8.148 | 1             | MoO <sub>4</sub> <sup>-2</sup> | 2 | Na <sup>+</sup> | 2  | H <sub>2</sub> O |   |                |

Table 33

Mass distribution of aqueous inorganic and organic species at pH=0.5 and  $I=0.2137$  from  $10^{-3}$  M CsNO<sub>3</sub> and 1 M NaNO<sub>3</sub> solution in presence of ZM as adsorbent ( $V/m = 100$  mL g<sup>-1</sup>)

| Component                      | Total dissolved | % dissolved | Total sorbed |
|--------------------------------|-----------------|-------------|--------------|
| =SOH(1)                        | 0               | 0.000       | 1.0024E-02   |
| Cs <sup>+</sup>                | 9.9319E-04      | 100.000     | 7.8959E-21   |
| H <sup>+</sup>                 | 1.7051E+15      | 100.000     | 2.0048E-02   |
| MoO <sub>4</sub> <sup>-2</sup> | 1.1368E+15      | 100.000     | 0            |
| Na <sup>+</sup>                | 3.6538E+00      | 100.000     | 7.7525E-17   |
| NO <sub>3</sub> <sup>-</sup>   | 1.3840E+01      | 99.928      | 1.0024E-02   |

(MoO<sub>3</sub>(s), -8.000, 0.000), (Na<sub>2</sub>Mo<sub>2</sub>O<sub>7</sub>(s), -15.075, 1.522), (Na<sub>2</sub>MoO<sub>4</sub>(s), -7.075, -8.565), and (Na<sub>2</sub>MoO<sub>4</sub>·2H<sub>2</sub>O(s), -7.075, -8.299). On the other side, addition of NaNO<sub>3</sub> would enhance the formation of the following species: (H<sub>2</sub>MoO<sub>4</sub>(s), -8.000,

4.876), (MoO<sub>3</sub>(s), -8.000, 0.000), (Na<sub>2</sub>Mo<sub>2</sub>O<sub>7</sub>(s), -14.924, 1.672), (Na<sub>2</sub>MoO<sub>4</sub>(s), -6.924, -8.414, and (Na<sub>2</sub>MoO<sub>4</sub>·2H<sub>2</sub>O(s), -6.924 and 8.148). As could be noticed, H<sub>2</sub>MoO<sub>4</sub>(s), Na<sub>2</sub>Mo<sub>2</sub>O<sub>7</sub>(s) are insoluble species, while MoO<sub>3</sub> is in equilibrium with the solution under these conditions.

#### 3.4.4. Thermodynamic of adsorption

In technological practice, thermodynamic variables such as enthalpy change ( $\Delta H^\circ$ ), entropy change ( $\Delta S^\circ$ ), and free energy change ( $\Delta G^\circ$ ) are crucial and must be taken into consideration in order to determine the spontaneity of a process. These parameters were obtained from adsorption experiments at various temperatures, namely, at 298, 308, 318, and 333 K using the following equations [45]:

$$K_c = \frac{C_i - C_e}{C_e} \quad (31)$$

Table 34

Formation constants and the related enthalpies of formation for inorganic and organic species at pH=0.5 and  $I=0.2137$  from  $10^{-3}$  M CsNO<sub>3</sub> and 1 M NaNO<sub>3</sub> solution in presence of ZM as adsorbent ( $V/m = 100$  mL g<sup>-1</sup>)

| Component  | log K   | $\Delta H$ (kJ mol <sup>-1</sup> ) | Stoichiometry   |                |                  |                                |                                   |                 |
|--|---------|------------------------------------|-----------------|----------------|------------------|--------------------------------|-----------------------------------|-----------------|
|  |         |                                    | Cs <sup>+</sup> | H <sup>+</sup> | H <sub>2</sub> O | MoO <sub>4</sub> <sup>-2</sup> | N (NO <sub>3</sub> <sup>-</sup> ) | Na <sup>+</sup> |
| CsNO <sub>3</sub> (aq)                                       | 0.02    | 0                                  | 1               | 0              | 0                | 0                              | 1                                 | 0               |
| H <sub>2</sub> Mo <sub>6</sub> O <sub>21</sub> <sup>-4</sup> | 51.17   | -218                               | 0               | 8              | -3               | 6                              | 0                                 | 0               |
| H <sub>3</sub> Mo <sub>8</sub> O <sub>28</sub> <sup>-5</sup> | 69.74   | -275                               | 0               | 11             | -4               | 8                              | 0                                 | 0               |
| HMo <sub>7</sub> O <sub>24</sub> <sup>-3</sup>               | 58.58   | -248                               | 0               | 9              | -4               | 7                              | 0                                 | 0               |
| HMoO <sub>4</sub> <sup>-</sup>                               | 4.24    | 22                                 | 0               | 1              | 0                | 1                              | 0                                 | 0               |
| Mo <sub>7</sub> O <sub>24</sub> <sup>-6</sup>                | 52.86   | -258                               | 0               | 8              | -4               | 7                              | 0                                 | 0               |
| Mo <sub>8</sub> O <sub>26</sub> <sup>-4</sup>                | 74.38   | -285                               | 0               | 12             | -6               | 8                              | 0                                 | 0               |
| MoO <sub>3</sub> (H <sub>2</sub> O) <sub>3</sub> (aq)        | 8.24    | -25                                | 0               | 2              | 0                | 1                              | 0                                 | 0               |
| NaNO <sub>3</sub> (aq)                                       | -0.55   | 0                                  | 0               | 0              | 0                | 0                              | 1                                 | 1               |
| NaOH (aq)  | -13.897 | 59.81                              | 0               | -1             | 1                | 0                              | 0                                 | 1               |
| OH <sup>-</sup>  | -13.997 | 55.81                              | 0               | -1             | 1                | 0                              | 0                                 | 0               |

Table 35

Effect competing ion concentration on the change in free energy of adsorption of <sup>134</sup>Cs<sup>+</sup>/ZM and <sup>134</sup>Cs<sup>+</sup>/ZIM

| Competing ion concentration | ΔG (kJ mole <sup>-1</sup> )        |        |                      |        |                                     |         |                      |        |
|-----------------------------|------------------------------------|--------|----------------------|--------|-------------------------------------|---------|----------------------|--------|
|                             | <sup>134</sup> Cs <sup>+</sup> /ZM |        |                      |        | <sup>134</sup> Cs <sup>+</sup> /ZIM |         |                      |        |
|                             | CH <sub>3</sub> COOH               | EDTA   | CH <sub>3</sub> COOH | EDTA   | CH <sub>3</sub> COOH                | EDTA    | CH <sub>3</sub> COOH | EDTA   |
| 1.00E-08                    | -7.928                             | -5.382 | -6.937               | -6.309 | -9.575                              | -10.312 | -7.529               | -7.041 |
| 1.00E-06                    | -7.755                             | -5.301 | -6.886               | -6.204 | -9.523                              | -10.399 | -7.437               | -6.886 |
| 1.00E-05                    | -5.725                             | -4.703 | -5.816               | -5.301 | -8.520                              | -8.997  | -6.643               | -6.103 |
| 1.00E-04                    | -5.636                             | -3.466 | -5.143               | -4.845 | -8.391                              | -8.112  | -5.816               | -6.044 |
| 1.00E-03                    | -5.465                             | -2.821 | -4.432               | -4.302 | -8.112                              | -6.886  | -5.301               | -6.005 |
| 1.00E-02                    | -4.845                             | -1.714 | -3.693               | -3.693 | -7.437                              | -5.143  | -4.302               | -4.703 |
| 1.00E-01                    | -4.565                             | -0.398 | -2.925               | -2.821 | -6.886                              | -4.175  | -4.432               | -4.050 |
| 1.00E+00                    | -4.175                             | 1.003  | -1.318               | -2.211 | -6.005                              | -3.031  | -1.516               | -3.246 |

$$\Delta_r G^\theta = -RT \ln K_c \tag{32}$$

$$\ln(K_c) = \frac{\Delta S^\theta}{R} - \frac{\Delta H^\theta}{RT} = -\frac{\Delta G^\theta}{RT} \tag{33}$$

where *K<sub>c</sub>* is the equilibrium constant. The values of Δ*H*<sup>θ</sup> and Δ*S*<sup>θ</sup> were obtained from the slope and intercept of van't Hoff plot of ln(*K<sub>c</sub>*) vs. 1/*T*. The use of van't Hoff plot is an indirect, but accurate method to calculate thermodynamic adsorption parameters at solid–solution interfaces. For accurate calculations, the real equilibrium constant and in turn the remaining thermodynamic parameters were computed using the activity results based on the Ibrahim-El-Gammal SSCCM.

According to the SSCCM, Tables 20, 24, 29, and 34 show the formation constants and the related enthalpies of formation for the inorganic and organic species at pH = 0.5 and *I* = 0.2137 from 10<sup>-3</sup> M CsNO<sub>3</sub> and 1 M CH<sub>3</sub>COOH, EDTA, NaCl, and NaNO<sub>3</sub> solutions, respectively, in presence of ZM as adsorbent

(*V*/*m* = 100 mL g<sup>-1</sup>). Few species such as HMoO<sub>4</sub><sup>-</sup> have a positive enthalpy of formation, while the remaining species are formed by exothermic reactions. Therefore, the comprehensive enthalpy change would be affected by the heat of formations of the species mentioned in those tables. Actually, the all-inclusive adsorption reactions are not enthalpy dependent; they are entropy directed. This fact is clearly seen in Tables 35 and 36 as the free energy of the different adsorption systems have negative values, which indicate the spontaneous nature of the system. The positive values of the entropy indicate the increasing randomness in the <sup>134</sup>Cs<sup>+</sup>/ZM system; at least 15–20 species are present in solution. Especially, Table 35 shows the effect competing ion concentration on the change in free energy of adsorption of <sup>134</sup>Cs<sup>+</sup>/ZM and <sup>134</sup>Cs<sup>+</sup>/ZIM. Negative free energies are generally encountered, which agrees with the continuous spontaneity of reactions. However, this spontaneous nature of adsorption decreases as the concentration of the ligand increases.

Table 36

Thermodynamic parameters for the adsorption of <sup>134</sup>Cs<sup>+</sup> on ZM and ZIM

| System                              | Temperature (K) | Δ <i>G</i> <sup>θ</sup> (kJ mol <sup>-1</sup> ) | Δ <i>H</i> <sup>θ</sup> (kJ mol <sup>-1</sup> ) | Δ <i>S</i> <sup>θ</sup> (J mol <sup>-1</sup> K) |
|-------------------------------------|-----------------|---|---|---|
| <sup>134</sup> Cs <sup>+</sup> /ZM  | 298             | -9.08068  | 36.546  | 135.87  |
|                                     | 308             | -7.5607   |   |   |
|                                     | 318             | -6.5164   |   |   |
|                                     | 333             | -6.328  |   |   |
| <sup>134</sup> Cs <sup>+</sup> /ZIM | 298             | -12.3019  | 45.256  | 165.894   |
|                                     | 308             | -8.69241  |   |   |
|                                     | 318             | -7.33028  |   |   |
|                                     | 333             | -7.136  |   |   |

#### 4. Conclusion

The sorption behavior of  $^{134}\text{Cs}^+$  onto ZM and ZIM under batch conditions after preparation and characterization of ZM and ZIM was carried out in the absence and presence of some complexing agents and some competing sodium ion. Based on Davis and Huckel Equations, the activities and the activity coefficients of the corresponding concentrations were calculated. Therefore, the different isothermal models were used to express the effect of concentration on the amount of  $^{134}\text{Cs}^+$  sorbed onto ZM and ZIM at a constant temperature in their real equilibrium conditions. A new model, SSCCM was developed based on 2-pK DLM to test several sets of data; applying the 2-pK basic Stern model and the TLM was not satisfactory. This is may be due to the high number of adjustable parameters involved in these model variations, which made the optimization procedure of the applied computer codes not to converge. Furthermore, a purely DLM generally gave the poorest fit to experimental data when combined with the 1-pK approach and was only slightly better when combined with the 2-pK formalism. The new SSCCM succeeded in explanation of the distinct sets of sorption data in different ionic strengths giving rise to the different activities, species, their distributions for both organic complexing ligands as acetic acid and EDTA and sodium as monovalent competing ion. The SSCCM explained the results of the solubility's of the inorganic species by calculation of their logarithmic ionic activity products and the corresponding saturation indices. Since the calculations in the SSCCM are based on the activities, the model could predict the real formation constants, and in turn, it could be clearly used to calculate the different thermodynamic parameters.

#### References

- [1] R.R. Reda, Synthesis and characterization of magnetic hexacyanoferrate (II) polymeric nanocomposite for separation of cesium from radioactive waste solutions, *J. Colloid Interface Sci.* 388(1) (2012) 21–30.
- [2] B. Pangen, H. Paudyal, K. Inoue, K. Ohto, H. Kawakita, S. Alam, Preparation of natural cation exchanger from persimmon waste and its application for the removal of cesium from water, *Chem. Eng. J.* 242 (2014) 109–116.
- [3] J.E. Mangold, C.M. Park, H.M. Liljestrand, L.E. Katz, Surface complexation modeling of Hg(II) adsorption at the goethite/water interface using the Charge Distribution Multi-Site Complexation (CD-MUSIC) model, *J. Colloid Interface Sci.* 418 (2014) 147–161.
- [4] H.B. Jung, S.T. Yun, J.S. Kwon, Y. Zheng, Role of iron colloids in copper speciation during neutralization in a coastal acid mine drainage, South Korea: Insight from voltammetric analyses and surface complexation modeling, *J. Geochem. Explor.* 112 (2012) 244–251.
- [5] E.M. Pecini, M.J. Avena, Measuring the isoelectric point of the edges of clay mineral particles: The case of montmorillonite, *Langmuir* 29(48) (2013) 14926–14934.
- [6] M.S. Azam, C.N. Weeraman, J.M. Gibbs-Davis, Halide-induced cooperative acid–base behavior at a negatively charged interface, *J. Phys. Chem. C* 117(17) (2013) 8840–8850.
- [7] H. Geckeis, J. Lützenkirchen, R. Polly, T. Rabung, M. Schmidt, Mineral–water interface reactions of actinides, *Chem. Rev.* 113(2) (2013) 1016–1062.
- [8] M.S. Azam, C.N. Weeraman, J.M. Gibbs-Davis, Specific cation effects on the bimodal acid–base behavior of the silica/water interface, *J. Phys. Chem. Lett.* 3(10) (2012) 1269–1274.
- [9] C.M. Jonsson, P. Persson, S. Sjöberg, J.S. Loring, Adsorption of glyphosate on goethite ( $\alpha\text{-FeOOH}$ ): Surface complexation modeling combining spectroscopic and adsorption data, *Environ. Sci. Technol.* 42(7) (2008) 2464–2469.
- [10] R. Chakravarty, S.K. Sarkar, M. Venkatesh, A. Dash, An electrochemical procedure to concentrate  $^{99m}\text{Tc}$  available from a zirconium [ $^{99}\text{Mo}$ ] molybdate gel generator, *Appl. Radiat. Isot.* 70(2) (2012) 375–379.
- [11] A. Magnaldo, M. Masson, R. Champion, Nucleation and crystal growth of zirconium molybdate hydrate in nitric acid, *Chem. Eng. Sci.* 62(3) (2007) 766–774.
- [12] B. El-Gammal, S.A. Shady, Chromatographic separation of sodium, cobalt and europium on the particles of zirconium molybdate and zirconium silicate ion exchangers, *Colloids Surf., A* 287(1–3) (2006) 132–138.
- [13] M.R. Davarpanah, S. Attar Nosrati, M. Fazlali, M. Kazemi Boudani, H. Khoshhosn, M. Ghannadi Maragheh, Influence of drying conditions of zirconium molybdate gel on performance of  $^{99m}\text{Tc}$  gel generator, *Appl. Radiat. Isot.* 67(10) (2009) 1796–1801.
- [14] F. Monroy-Guzmán, L.V. Díaz-Archundia, A. Contreras Ramírez, Effect of Zr:Mo ratio on  $^{99m}\text{Tc}$  generator performance based on zirconium molybdate gels, *Appl. Radiat. Isot.* 59(1) (2003) 27–34.
- [15] R.R. Sheha, S.H. El-Khouly, Adsorption and diffusion of cesium ions in zirconium(IV) iodomolybdate exchanger, *Chem. Eng. Res. Des.* 91(5) (2013) 942–954.
- [16] S.A. Nabi, S.A. Ganai, Mu Naushad, A new Pb $^{2+}$  ion selective hybrid cation exchanger-, EDTA–zirconium iodate: Synthesis, characterization and analytical applications, *AST* 26(6) (2009) 1.
- [17] I.M. Kolthoff, R. Belcher, *Volumetric Analysis*, vol. 3. Interscience, New York, NY, 1957.
- [18] B. Beena, A. Shivaneekar, U. Chudasama, Catalytic activity of Pd(II) sorbed on an inorganic ion exchanger—zirconium molybdate, *J. Mol. Catal. A: Chem.* 107 (1996) 347.
- [19] M.V. Sivaiah, S.S. Kumar, K.A. Venkatesan, R.M. Krishna, P. Sasidhar, G.S. Murthy, in: B.S. Tomar, M.K. Saxena, V.K. Manchanda, S.B. Manohar (Eds.), *Proceedings of the Nuclear and Radiochemistry Symposium*, Mumbai, vol. 10–13 February 2003, BARC, Mumbai (2003), p. 279.
- [20] R. Bates, *Determination of pH, Theory and Practice*, John Wiley, New York, NY, 1973, 479–489.
- [21] G. Sposito, *The Thermodynamics of Soil Solutions*, Clarendon Press, Oxford, UK, 1981.

- [22] H. Mimura, F. Tachibana, K. Akiba, Ion-exchange selectivity for cesium in ferrierites, *J. Nucl. Sci. Technol.* 29 (1992) 184–186.
- [23] Y.S. Ho, J.F. Porter, G. McKay, Equilibrium isotherm studies for the sorption of divalent metal ions on to peat: copper, nickel and lead single component systems, *Water Air Soil Pollut.* 141 (2002) 1–33.
- [24] A. Ebadi, J.S. Soltan Mohammadzadeh, A. Khudiev, What is the correct form of BET isotherm for modeling liquid phase adsorption? *Adsorption* 15 (2009) 65–73.
- [25] Z. Benmaamar, A. Bengueddach, Correlation with different models for adsorption isotherms of M-xylene and toluene on zeolites, *J. Appl. Sci. Environ. Sanit.* 2 (2007) 43–56.
- [26] Sh Basha, B. Jha, Estimation of isotherm parameters for biosorption of Cd(II) and Pb(II) onto brown seaweed, *Lobophora ariegata*, *J. Chem. Eng. Data* 53 (2008) 449–455.
- [27] C. Alliot, L. Bion, F. Mercier, P. Toulhoat, Sorption of aqueous carbonic, acetic, and oxalic acids onto  $\alpha$ -alumina, *J. Colloid Interface Sci.* 287 (2005) 444–451.
- [28] G. Sposito, *The Environmental Chemistry of Aluminium*, Lewis Publishers, Boca Raton, FL, 1996, pp. 131–171.
- [29] G. Sposito, *The Environmental Chemistry of Aluminium*, Lewis Publishers, Boca Raton, FL, 1996, pp. 184–189.
- [30] J. Lützenkirchen, The constant capacitance model and variable ionic strength: An evaluation of possible applications and applicability, *J. Colloid Interface Sci.* 217 (1999) 8–18.
- [31] W. Stumm, C.P. Huang, S.R. Jenkins, Specific chemical interactions affecting the stability of dispersed systems, *Croat. Chem. Acta* 42 (1970) 223–244.
- [32] C.P. Huang, W. Stumm, Specific adsorption of cations on hydrous  $\gamma$ - $\text{Al}_2\text{O}_3$ , *J. Colloid Interface Sci.* 43 (1973) 409–420.
- [33] R.J. Hunter, *Zeta Potential in Colloid Science, Principles and Applications*, Academic Press, London, 1981.
- [34] F. Booth, The dielectric constant of water and the saturation effect, *J. Chem. Phys.* 19 (1951) 391–394.
- [35] M. Flörsheimer, K. Kruse, R. Polly, A. Abdelmonem, B. Schimmelpfennig, R. Klenze, T. Fanghänel, Hydration of mineral surfaces probed at the molecular level, *Langmuir* 24 (2008) 13434–13439.
- [36] A. Breeuwsma, J. Lyklema, Physical and chemical adsorption of ions in electrical double-layer on hematite ( $\alpha$ - $\text{Fe}_2\text{O}_3$ ), *J. Colloid Interface Sci.* 43 (1973) 437–448.
- [37] F. Adekola, M. Fédoroff, H. Geckeis, T. Kupcik, G. Lefèvre, J. Lützenkirchen, M. Plaschke, T. Preocanin, T. Rabung, D. Schild, Characterization of acid–base properties of two gibbsite samples in the context of literature results, *J. Colloid Interface Sci.* 354 (2011) 306–317.
- [38] A. Naveau, F. Monteil-Rivera, J. Dumonceau, S. Boudesocque, Sorption of europium on a goethite surface: Influence of background electrolyte, *J. Contam. Hydrol.* 77 (2005) 1–16.
- [39] J. Jiang, R.K. Xu, S.Z. Li, Effect of ionic strength and mechanism of Cu(II) adsorption by goethite and  $\gamma$ - $\text{Al}_2\text{O}_3$ , *J. Chem. Eng. Data* 55 (2010) 5547–5552.
- [40] W. Stumm, J.J. Morgan, *Chemical Equilibria and Rates in Natural Waters*, Aquatic Chemistry Wiley Interscience, third ed., Wiley-Interscience, New York, NY, 1996.
- [41] M.S. Schaller, C.M. Koretsky, T.J. Lund, C.J. Landry, Surface complexation modeling of Cd(II) adsorption on mixtures of hydrous ferric oxide, quartz and kaolinite, *J. Colloid Interface Sci.* 339(2) (2009) 302–309.
- [42] W.D. Schecher, D.C. McAvoy, *MINEQL+: User's Manual*, Environmental Research Software, Edgewater, Hallowell, ME, 2001.
- [43] D.A. Dzombak, F.M.M. Morel, *Surface Complexation Modeling: Hydrous Ferric Oxide*, John Wiley, New York, NY, 1990.
- [44] T. Xu, *TOUGHREACT Testing in High Ionic Strength Brine Sandstone Systems*, Lawrence Berkeley National Laboratory, Berkeley, CA, LBNL Paper, LBNL-1051E, 2008.
- [45] A. Kamari, W.S. Ngah, Isotherm, kinetic and thermodynamic studies of lead and copper uptake by  $\text{H}_2\text{SO}_4$  modified chitosan, *Colloids Surf., B* 73 (2009) 257–266.